sustainability

MDPI

Article

GIS-Based Site Selection for Agricultural Water Reservoirs: A Case Study of São Brás de Alportel, Portugal

Olga Dziuba [1], Cláudia Custódio [2], Carlos Otero Silva [3,4], Fernando Miguel Granja-Martins [3,5], Rui Lança [3] and Helena Maria Fernandez [3,5,*]

[1] GeoPole-Engineering Surveying, Kievskaya Street, Building 16, Apt. 26, 121165 Moscow, Russia; od@geopole.ru
[2] Câmara Municipal de São Brás de Alportel, 8150-151 São Brás de Alportel, Portugal; claudia.custodio@cm-sbras.pt
[3] Departamento de Engenharia Civil, Instituto Superior de Engenharia, Universidade do Algarve, 8005-139 Faro, Portugal; csilva@ualg.pt (C.O.S.); fmmartin@ualg.pt (F.M.G.-M.); rlanca@ualg.pt (R.L.)
[4] MED Mediterranean Institute for Agriculture, Environment and Development & CHANGE Global Change and Sustainability Institute, Institute for Advanced Studies and Research, Universidade de Évora, 7000-083 Évora, Portugal
[5] Centre for Research in Tourism, Sustainability and Well-Being (CinTurs), Universidade do Algarve, 8005-139 Faro, Portugal
* Correspondence: hfernand@ualg.pt

Abstract

In the São Brás de Alportel municipality, water scarcity poses a significant constraint on agricultural activities. This study utilises Remote Sensing (RS) and Geographical Information Systems (GISs) to identify existing irrigated areas, delineate catchment basins, and select the most suitable sites for the installation of new surface water reservoirs. First, the principal territorial components were characterised, including physical elements (climate, geology, soils, and hydrography) and anthropogenic infrastructure (road network and high-voltage power lines). Summer Sentinel-2 satellite imagery was then analysed to calculate the Normalised Difference Vegetation Index (NDVI), enabling the identification and classification of irrigated agricultural parcels. Flow directions and accumulations derived from Digital Elevation Models (DEMs) facilitated the characterisation of 38 micro-catchments and the extraction of 758 km of the drainage network. The siting criteria required a minimum setback of 100 m from roads and high-voltage lines, excluded farmland currently in use, and favoured mountainous areas with low permeability. Only 18.65% (2854 ha) of the municipality is agricultural land, of which just 4% (112 ha) currently benefits from irrigation. The NDVI-based classification achieved a Kappa coefficient of 0.88, indicating high reliability. Three sites demonstrated adequate storage capacity, with embankments measuring 8 m, 10 m, and 12 m in height. At one of these sites, two reservoirs arranged in a cascade were selected as an alternative to a single structure exceeding 12 m in height, thereby reducing environmental and landscape impact. The reservoirs fill between October and November in an average rainfall year and between October and January in a dry year, maintaining a positive annual water balance and allowing downstream plots to be irrigated by gravity. The methodology proved to be objective, replicable, and essential for the sustainable expansion of irrigation within the municipality.

Keywords: Geographic Information Systems (GISs); water balance; irrigation; reservoirs

Academic Editor: Lia Bárbara Cunha Barata Duarte

Received: 15 September 2025
Revised: 1 November 2025
Accepted: 7 November 2025
Published: 17 November 2025

Citation: Dziuba, O.; Custódio, C.; Silva, C.O.; Granja-Martins, F.M.; Lança, R.; Fernandez, H.M. GIS-Based Site Selection for Agricultural Water Reservoirs: A Case Study of São Brás de Alportel, Portugal. *Sustainability* **2025**, *17*, 10276. https://doi.org/10.3390/su172210276

1. Introduction

Mediterranean agricultural systems are facing an urgent water scarcity problem due to climate change, highly irregular rainfall, and increasing competition for water resources. In the Algarve region, annual precipitation averages around 560 mm, primarily occurring during the wet half-year. However, the hottest months often result in severe water deficits that compromise crop productivity, rendering rainfed agriculture increasingly unsustainable [1,2]. Severe drought episodes in 1993, 2005, 2012, and 2019, confirmed by the Palmer Drought Severity Index (PDSI) published by the Portuguese Institute for Sea and Atmosphere, illustrate the vulnerability of these systems, with a worsening trend observed in the monthly bulletins for 2023. Efficient water management, including reservoir planning and irrigation optimisation, is therefore essential to maintain agricultural sustainability and resilience [3].

Anthropogenic activities, particularly the combustion of fossil fuels, intensify global warming and amplify the effects of climate change, which now constitute the foremost threat to sustainable development in the twenty-first century, impacting all three pillars, namely, environmental, economic, and social [4]. These impacts manifest as extreme meteorological events, droughts, and floods that compromise the resilience of agricultural systems; in Mediterranean-type regions, characterised by highly irregular rainfall, such uncertainty becomes especially critical [1]. Societal sustainability, therefore, hinges on the judicious management of natural resources, particularly water, the basis of life and every productive chain [5]. Agriculture offers the most significant scope for improving water-use efficiency among economic sectors, whether through refinements infield practice or internalising water use's environmental cost [6].

Remote Sensing (RS) and Geographic Information Systems (GISs) are fundamental in fostering a more modern and sustainable agriculture, characterised by markedly more efficient water management. These tools enable precise crop mapping, reliable estimation of water requirements, and informed irrigation scheduling, thereby optimising water resources and reducing wastage [7]. Numerous studies based on Sentinel-2 imagery demonstrate that Convolutional Neural Networks and machine-learning time series analyses can accurately identify irrigated areas and monitor land use, soil moisture, and water stress [8–10].

Digital Elevation Models (DEMs) and GISs provide critical support for hydrological analysis by modelling flow direction and accumulation, delineating catchment boundaries, and identifying optimum sites for water retention [11,12]. More recent literature incorporates specialised agro-hydrological tools, such as the MHYDAS-Small-Reservoirs module, which integrates hydro-sedimentary dynamics in a chain of reservoirs typical of Mediterranean basins [13]. Refined evaporative-balance models for small dams quantify losses exceeding 25% of the annual volume under a regional warming of +2 °C [14]. Participatory approaches have demonstrated the socio-economic viability of cascaded reservoir systems in Tuscany and Andalusia, integrating local governance, water-use efficiency, and ecosystem conservation [15].

The São Brás de Alportel case study analysed here exemplifies these synergies. The municipality occupies an area between the *Barrocal* and *Serra* zones. In the northern *Serra*, higher elevations, steep slopes, and shallow, schistose soils limit agricultural activity. In contrast, the southern *Barrocal* is flatter, underlain by calcareous soils, and is more suitable for agriculture, particularly rainfed crops and orchards. The municipality lies across two drainage basins: the Algarve Coastal Streams basin and the Guadiana River basin. These basins are crucial for water supply, climate regulation, and environmental sustainability, directly impacting local livelihoods and the regional economy. The municipality is also

served by a road network that ensures access to rural areas and potential reservoir sites, including National Road EN-2 and Municipal Road EM-270.

Using 25 cm-resolution orthophotos, cadastral data, and Sentinel-2 imagery, 2854 ha of agricultural land were mapped, of which only 112 ha are irrigated, identified via the Normalised Difference Vegetation Index (NDVI) with a Kappa coefficient of 0.88. Hydrological modelling based on the DEM and interpolated rainfall data delineated 38 micro-catchments and selected three sites with suitable geomorphological conditions for small dams with 8 m to 12 m high. At one of these sites, two reservoirs arranged in a cascade were selected as an alternative to a single structure exceeding 12 m in height, thereby reducing environmental and landscape impact. The water-balance assessment indicated complete reservoir recharge between October and November in an average year and between October and January in a dry year, meeting agricultural demand during the summer. It also suggested the construction of additional downstream reservoirs to harness surplus discharges. This cascaded solution reconciles risk mitigation, reduces landscape impact, and provides gravity-fed water distribution, eliminating the need for pumping energy to supply the agricultural plots.

In light of the above, this study addresses the need to enhance water resilience in the region by identifying the most suitable locations for agricultural water reservoirs. The approach relies on the integration of three scientific domains central to the sustainable management of water resources: (i) high-resolution multispectral remote sensing for monitoring land use and efficiency; (ii) Geographic Information Systems (GISs) combined with a criteria-based spatial evaluation framework for decision support; and (iii) hydrological modelling capable of simulating catchment behaviour under different scenarios of hydrological variability. Within this integrated framework, the specific objectives are as follows: (i) to identify locations most suitable for constructing agricultural reservoirs in a Mediterranean context by combining biophysical and territorial criteria using GISs and remote sensing; (ii) to calculate the water balance of each contributing catchment to inform storage capacity estimates; and (iii) to propose a structured, transferable methodology that can be applied in other territories facing increasing water stress.

2. Materials and Methods

2.1. Study Area

The municipality of São Brás de Alportel (Figure 1) occupies 153.4 km^2 and lies between the Barrocal and the Serra zones (37°16′–37°07′ N, 7°47′–7°58′ W; Figure 1). In the north of the municipality, the Serra is characterised by higher elevations, steeper slopes, and predominantly schistose, shallow, sometimes skeletal soils. The land cover is primarily forested, with the cork oak (*Quercus suber*) as the dominant species.

In contrast, the southern Barrocal is generally flatter, underlain by calcareous soils. It is typified by stands of carob (*Ceratonia siliqua*), which, although classified as a forest species, is commonly associated with rainfed orchard systems of fig (*Ficus carica*), almond (*Prunus dulcis*), and olive (*Olea europaea*).

For this study, agricultural areas were delineated using the Portuguese Land Use and Land Cover Map (COS 2018, scale 1:25,000), the 2019 Cadastral Survey (scale 1:10,000), both produced by Direção Geral do Território (DGT), Portugal, and the 2020 Topographic Base Map (scale 1:10,000) produced by São Brás de Alportel Municipal Council (SBAMC). Approximately 27.3 km^2 of the municipality is occupied by rainfed systems, whereas 1.6 km^2 supports irrigated crops. Areas under fruit trees, vineyards, olive groves, and vegetable plots cover 9.6 km^2, 0.6 km^2, 14.4 km^2, and 42.8 km^2, respectively.

The climate is Mediterranean with Atlantic influence. According to the Köppen–Geiger classification, it is warm temperate with dry, hot summers (Csa) [16]. Mean annual

precipitation is about 560 mm, falling chiefly in the cooler months, while the mean annual temperature is 16.1 °C.

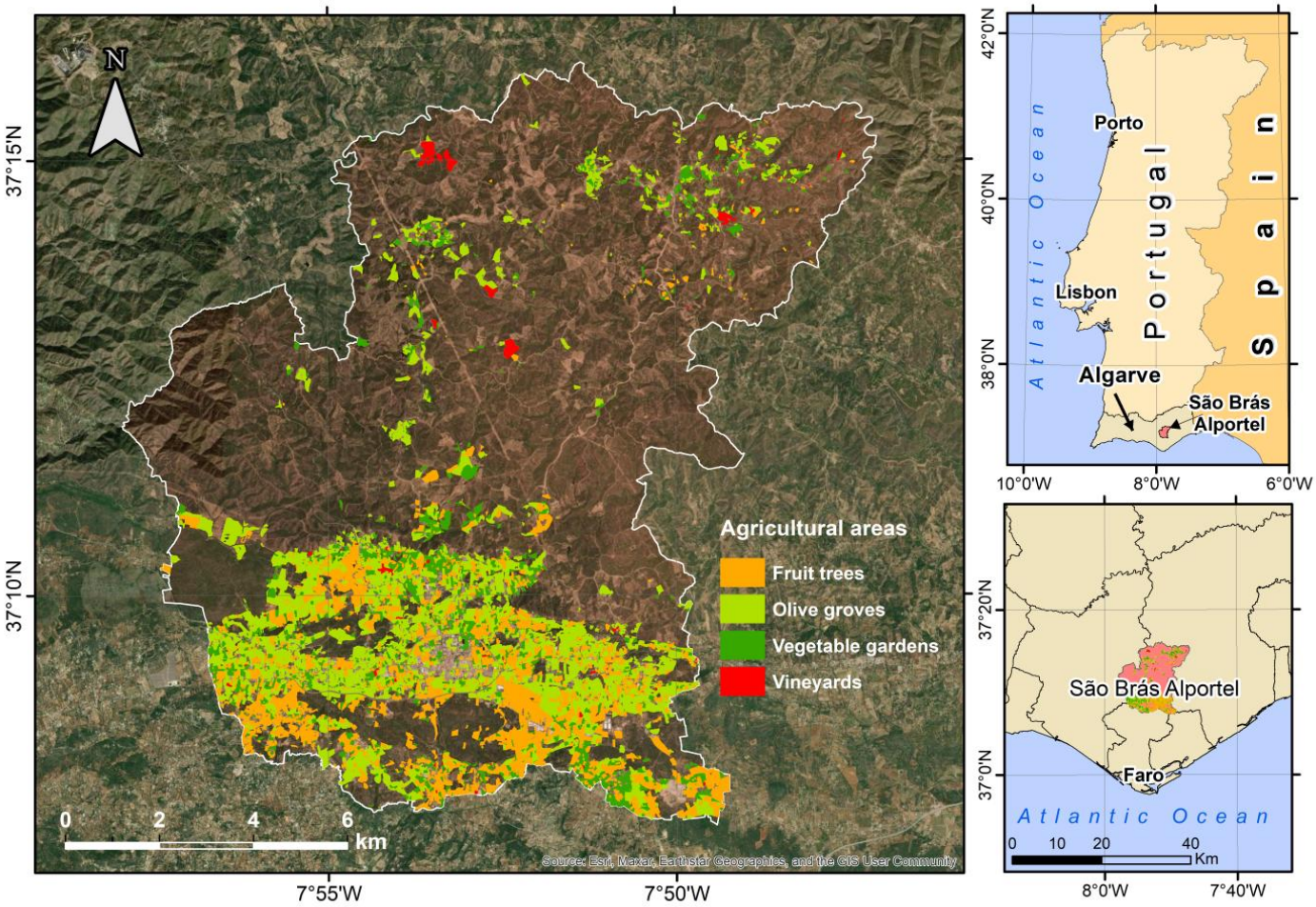

Figure 1. Boundary of the Municipality of São Brás de Alportel showing agricultural land use.

Soils in the Serra are skeletal, agriculturally unsuitable, predominantly schistose, and associated with an irregular relief. By contrast, the Barrocal is underlain by calcareous soils with gentler, less rugged topography, where limestone hills support Mediterranean vegetation [17]. Agricultural activity is therefore viable only within the Barrocal zone.

The municipality of São Brás de Alportel is situated between two drainage basins: the Algarve Coastal Streams basin (61.5% of the municipal area) and the Guadiana River basin (38.5%). The territory is also drained by several minor watercourses, notably the Ribeira de Alportel (the most important), Ribeira de Fronteira, Ribeira de Odeleite, Ribeira das Ruivas, Ribeira das Mercês, Ribeira da Ameixeira, Ribeira das Pernadas, Ribeira da Gaifona, Ribeira do Centianes, Ribeira do Peral, Ribeira do Barranquinho, Ribeira das Ondas, and Ribeira do Fialho. Also overlies two groundwater bodies: the São Brás de Alportel Aquifer System and the Peral–Moncarapacho Aquifer System.

Given the hydrological constraints and the need to manage water resources effectively, accessibility throughout the municipality is essential to support this management. The network of principal roads ensures connectivity: the National Road EN-2 links São Brás de Alportel to other parts of the country, while the Municipal Road EM-270 interconnects urban and rural areas and neighbouring localities, facilitating access for agricultural activities, reservoir construction, and maintenance. Figure 2 presents the hydrological and road networks of the municipality.

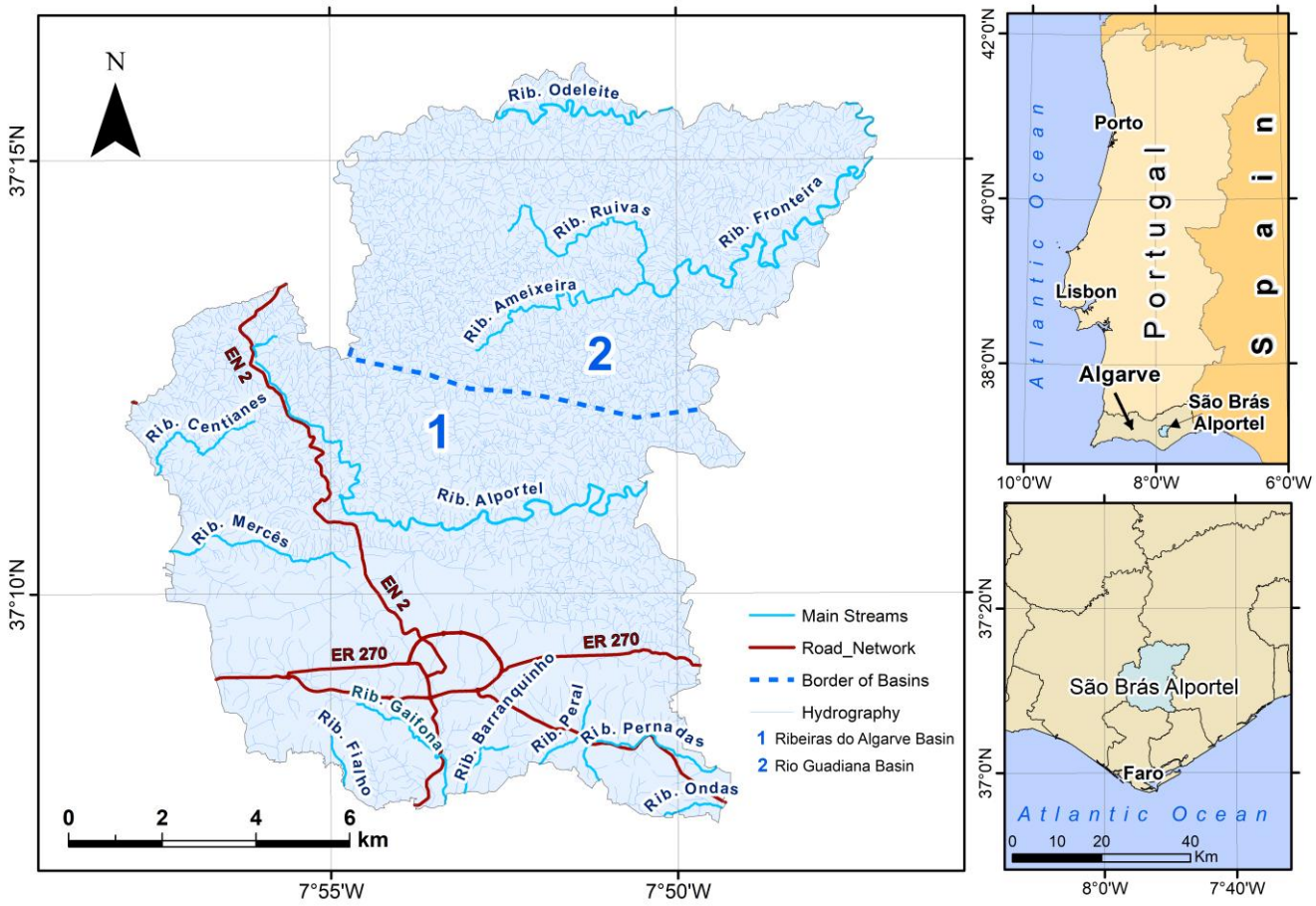

Figure 2. Hydrographic and Road Networks of the Municipality of São Brás de Alportel.

2.2. GIS Methodology

It was first necessary to delineate the municipality's agricultural land to identify potential sites for constructing water reservoirs. Polygons representing agricultural areas were extracted from the base topographic map. These polygons were subsequently refined using 29 RGB orthophotos from July 2021 with a spatial resolution of 25 cm, also provided SBAMC, and through field visits, to remove non-agricultural features such as dwellings, swimming pools, and other structures. The refined polygons were then intersected with the agricultural subclasses of COS 2018, which distinguish between temporary rainfed and irrigated crops, permanent crops (such as orchards and olive groves), and heterogeneous agricultural areas. COS 2018 had previously been corrected to exclude buildings and road networks.

Irrigated agricultural areas were identified using a multi-temporal *NDVI* analysis derived from Sentinel-2 imagery (Equation (1)) [18].

$$NDVI = \frac{NIR - R}{NIR + R} \quad (1)$$

where R represents the Red band (665 nm) and NIR the Near-Infrared band (842 nm).

Satellite images from June, July, August, and September 2021 were retrieved from Google Earth Engine (GEE), with a cloud cover threshold of less than 10%. These summer months were selected because rainfall is minimal in the Algarve, allowing elevated *NDVI* values to be confidently attributed to irrigation activity.

The analysis was restricted to agricultural parcels only, and the mean *NDVI* was calculated across the four months. This *NDVI* layer was subsequently reclassified into

five classes (0–0.1, 0.1–0.2, 0.2–0.4, 0.4–0.7, 0.7–1.0) to reflect vegetation vigour and irrigation intensity.

Some irrigated parcels were known a priori, while other areas with uncertain irrigation status were verified through four field visits. These field-verified parcels corresponded to *NDVI* values in the range 0.40–0.71, which were then used to classify irrigated areas across the study region.

By Portuguese regulation no. 202/70 Article 57 [19], the minimum unit of area qualifying as irrigated horticultural land in the district of Faro is 0.5 ha. A parcel was considered irrigated if it contained at least 0.5 ha of pixels with *NDVI* values within the 0.40–0.71 range.

A confusion matrix was constructed to validate the irrigation/non-irrigation classification by comparing classified pixels with reference pixels. A total of 100 samples were randomly selected within agricultural parcels and validated in the field using a Leica Zeno FLX100 Plus antenna in RTK mode. Subsequently, omission and commission errors and Cohen's Kappa (κ) coefficient were computed. Classification accuracy categories are based on k, as follows [20], and are presented in Table 1.

Table 1. Cohen's Kappa classification Accuracy.

k (%)	Classification Accuracy
<0	Poor
[0; 20[	Slight
[20; 40[	Fair
[40; 60[	Moderate
[60; 80[	Substantial
[80; 100]	Almost perfect

For clarity, Table 2 summarises all datasets used in this study, including their type, spatial resolution, temporal coverage, and source.

Table 2. Summary of datasets used in this study.

Dataset/Source	Data Type	Spatial Resolution	Temporal Coverage/Year	Notes
COS 2018-DGT	Vector	1:25,000 (~5 m)	2018	Delineation of agricultural areas
Cadastral Survey 2019-DGT	Vector	1:10,000 (~2 m)	2019	Parcels and property boundaries
Topographic Base Map 2020-SBAMC	Vector	1:10,000 (~2 m)	2020	Municipal boundaries, roads, rivers
RGB Ortophotos July 2021-SBAMC	Raster	25 cm	July 2021	Refinement of polygons, removal of dwellings, swimming pools, and other structures
Sentinel 2-GEE	Raster	10 m (Red and NIR bands)	June-September 2021	Multi-temporal imagery used for NDVI calculation, cloud cover <10%
Field Validation Points	Vector	GNSS-RTK (Multifrecuencia): <2 cm + 1 ppm	September	100 points for the confusion matrix

2.2.1. Most Suitable Sites for Agricultural Reservoirs

The most suitable sites for agricultural water-supply reservoirs were identified based on five criteria:

(i) Proximity to the drainage network (up to 10 m) and setback from infrastructure (more than 100 m from roads and high-voltage power lines);
(ii) Location on preferentially impermeable soils;
(iii) Location outside existing agricultural parcels and outside designated construction zones;
(iv) The reservoir site should be situated in a narrow valley with steep slopes, where the upstream section widens, allowing the formation of a sufficiently large water body for storage, while keeping the water depths between 8 m and 12 m and maintaining the

inundated area as small as possible, thus minimising impacts on protected habitats and species;

(v) The reservoir crest should be located as close as possible to the first agricultural area to be served.

2.2.2. Digital Elevation Model and Drainage Derivation

The DEM was created based on elevation points, contour lines, and hydrography obtained from a 1:10,000 scale topographic map. The model was generated with a spatial resolution of 10 m using the Triangulated Irregular Network (TIN) method with linear interpolation. This interpolation approach was considered appropriate given that, in most of the study area, slopes are relatively smooth and linear in cross-section, particularly in the southern sector where terrain variability is low. The DEM was corrected for sinks, and flow direction and accumulation models were calculated.

A drainage line was created for flow-accumulation values greater than 160 cells. This ArcGIS 10.8 (Esri, Redlands, CA, USA) hydrological parameter indicates the number of upstream raster cells draining to each location, thereby indicating where water tends to concentrate. The threshold was validated in the field by identifying a minor watercourse that the model confirmed at that accumulation value. Stream orders were assigned using the Strahler method, and the associated micro-catchments were delineated.

To preserve network connectivity for subsequent flow analyses, drainage elements were converted to a vector Geometric Network with downstream flow directions explicitly defined, an essential framework for locating reservoirs.

2.2.3. Micro-Catchment Delineation and Site Criteria

Micro-catchments were defined for all streams in the study area. For each candidate reservoir, the downstream drainage area and its flowline were delineated.

Additional siting criteria stipulated a 100 m buffer from roads and power lines, avoidance of land currently under cultivation, and preference for mountainous terrain with low permeability and adequate storage potential. Potential sites were limited to locations suitable for embankments up to 12 m high that would fill between January and February, maintain a positive annual water balance and permit gravity-fed irrigation of downstream parcels situated within 10 m of the channel.

2.3. Water Balance

2.3.1. Water-Balance Equations for a Cascade of Reservoirs

The water balance of a reservoir is defined by the relationship between the volume of water entering, the volume leaving and the change in stored water over a given period. Calculating this balance requires quantifying the hydrological processes involved—namely precipitation, evapotranspiration, evaporation and surface runoff. The hydrological balance of a reservoir [21] for a specified time interval is expressed by Equation (2).

$$\Delta V = V_{in} - V_{out} \quad (2)$$

where ΔV is the change in stored volume (m^3), V_{in} is the inflow volume (m^3), and V_{out} is the outflow volume (m^3). The inflow volume was calculated with Equation (3).

$$V_{in} = R \times A_{basin} + V_m \quad (3)$$

where R is the monthly surface-runoff depth (m); A_{basin} the upstream catchment area, less the area contributing to the reservoir immediately upstream on the same watercourse, where applicable (m^2); and V_m the volume discharged by that upstream reservoir (where applicable).

The outflow volume was calculated with Equation (4).

$$V_{out} = ET \times A_r + D + E \quad (4)$$

where ET is the evapotranspiration (m), A_r is the irrigated agricultural area (m^2), D *is* the emergency spill discharge released when the reservoir reaches its maximum capacity, and E is the direct evaporation from the reservoir surface.

2.3.2. Water Productivity of the Catchments

In the upstream catchment, water productivity is primarily governed by three hydrological processes: precipitation, soil water retention, and surface runoff. For the present study, runoff data were obtained from the River Basin Management Plan for the Algarve Region, provided by the Portuguese Environmental Agency (APA) [22].

According to APA [22], for Water Region 8 (Algarve Coastal Streams), surface water availability under natural conditions was assessed through hydrological modelling, producing monthly runoff series derived from precipitation and potential evapotranspiration data. A distributed grid-based model with 1 km spatial resolution and monthly time steps, implementing the Temez water balance method, was employed. Monthly precipitation and mean temperature datasets were used to generate spatially distributed estimates of potential and actual evapotranspiration, aquifer recharge, and total runoff. Model outputs were stored by sub-catchment and were driven by topographic, soil, meteorological and land use data, calibrated for the period 1930–2015 in part 2—volume B—Characterisation and Assessment [22].

Monthly runoff data for the Arade catchment (the adjacent area extending from São Bartolomeu de Messines to Alte; Table 3) were used. This choice was justified because the precipitation regimes and geology/soils of the two regions are identical, and they do not provide runoff data explicitly for the catchments examined in this study [22]. The APA Environmental Atlas [23] likewise shows that the annual runoff value is the same for both the Arade Basin and the study area (Figure 3).

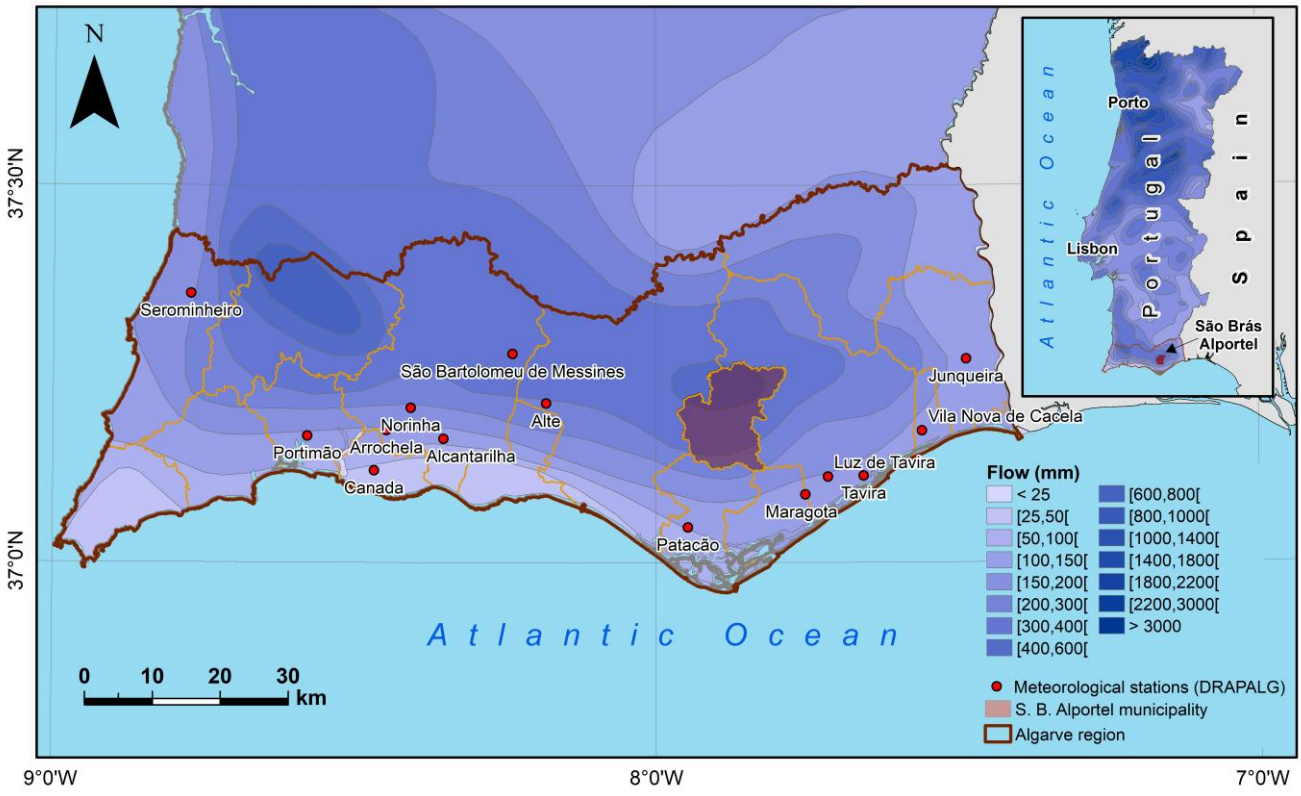

Figure 3. Mean annual runoff derived from [23].

Table 3. Monthly natural runoff (R) values for the Arade subbasin in mm for the average year and dry year [22].

	Oct	Nov	Dec	Jan	Feb	Mar	Apr	May	Jun	Jul	Aug	Sep
Average	18.4	32.7	50.1	46.0	35.8	29.6	14.3	7.2	2.0	1.0	1.0	2.0
Dry	1.0	3.1	5.1	6.1	6.1	4.1	4.1	2.0	1.0	0.5	0.2	0.2

According to APA [22], a dry year is characterised by a systematic reduction in monthly precipitation compared to the average year, with this reduction ranging from approximately −97% in August to −61% in March. This classification was derived from the analysis of long-term rainfall and runoff series, corresponding roughly to the lower quartile (P25) of the hydrological reference period. The average and dry years are used in hydrological and water-balance modelling to simulate scenarios of regular and reduced water availability for surface reservoirs, groundwater recharge, and agricultural water demand.

2.3.3. Water Losses from the Reservoirs

Water losses from reservoirs occur through direct evaporation and infiltration. In the present study, infiltration losses were assumed to be negligible. However, evaporation losses were estimated from monthly pan-evaporation data recorded at the São Brás de Alportel meteorological station of the National Water Resources Information System (SNIRH) [24] and multiplied by a pan coefficient of 0.7 [25]. Mean monthly pan-evaporation values for the period 1978–2018 are given in Table 4.

Table 4. Mean monthly pan evaporation in mm [24].

Oct	Nov	Dec	Jan	Feb	Mar	Apr	May	Jun	Jul	Aug	Sep
106.0	61.6	58.1	45.8	57.3	102.5	113.3	149.1	202.4	257.5	232.6	163.4

2.3.4. Irrigation Water Requirements

Irrigation water requirements are determined by the irrigated area and crop evapotranspiration, as expressed by Equation (5) [25].

$$ET_c = ET_o \times K_c \times K_s \quad (5)$$

where *ETo* is the reference evapotranspiration, K_c is the crop coefficient, and K_s is the water-stress coefficient; irrigation is assumed to occur under non-stress conditions, so $K_s = 1$.

The potential evapotranspiration (*ETo*) data were obtained from APA [22], where *ETo* was estimated based on air temperature using the Hargreaves method, selected due to the wider availability and reliability of temperature records (Table 5).

Table 5. Monthly reference-evapotranspiration data expressed as the mean of monthly records from APA [22] for the period 1930–2015, in mm.

Oct	Nov	Dec	Jan	Feb	Mar	Apr	May	Jun	Jul	Aug	Sep
83.0	49.0	39.0	43.0	52.0	87.0	100.0	137.0	163.0	185.0	168.0	123.0

The crop coefficients (*Kc*) used in this study are those published by [2]. In line with the agricultural systems present, four *Kc* categories were defined: orchard (citrus), olive grove, table-grape vineyard (Table 6), and small vegetable crops.

For kitchen-garden plots, the crop coefficient value of 1.05 recommended by [25] for small vegetables was adopted.

The *Kc* value used in calculating *ETc* corresponded to the area-weighted mean of the *Kc* values for those crop areas that intersect the watercourse downstream of the reservoir.

Table 6. Crop coefficients [2].

	Oct	Nov	Dec	Jan	Feb	Mar	Apr	May	Jun	Jul	Aug	Sep
Citr.	0.67	0.67	0.76	0.72	0.72	0.66	0.67	0.66	0.67	0.66	0.66	0.66
Oliv.	0.68	0.78	0.64	0.62	0.62	0.65	0.61	0.56	0.55	0.54	0.54	0.57
Vin.	0.45	0	0	0	0	0.25	0.45	0.6	0.7	0.7	0.85	0.55

Cit. = Citrus; Oliv. = Olive; Vin. = Vineyard.

2.3.5. Criteria for Determining Reservoir Volume

The minimum usable volume of the reservoirs is determined by the upstream catchment area at the dam site, the irrigated area supplied by the reservoir, and local data on runoff and evapotranspiration. Thus, neglecting direct reservoir losses through infiltration and evaporation, we obtain the following:

$$R \times A_b - ET_c \times A_r = \Delta V \tag{6}$$

where

$$k = A_b / A_r \tag{7}$$

gives

$$\Delta V_i = A_b \times \left(R_i - \frac{ET_{ci}}{k} \right),\ i = Oct,\ Nov,\ Dec,\ Jan,\ \ldots,\ Sep \tag{8}$$

$$Vol. = \sum_{\substack{i=Jan \\ \Delta V_i<0}}^{i=Dec} \Delta V_i \tag{9}$$

where R is the runoff (m); A_b is the upstream catchment area at the dam site (m^2); ET_c is the crop evapotranspiration (m), calculated as = $ET_o \times K_c$; ET_o is the reference evapotranspiration (m); K_c is the crop coefficient; A_r is the irrigated area supplied by the reservoir (m^2); ΔV is the monthly change in volume (m^3); *Vol.* is the minimum usable volume of the reservoir, defined as modulus of the sum of the negative monthly variations, typically occurring in the summer months (m^3).

The monthly water balance begins in October, when stored water volumes are at their lowest, and ends in September, coinciding with the onset of the wet semester and the start of the hydrological year.

From Equation (9), it is therefore possible to plot curves of the minimum usable reservoir volume per square kilometre of upstream catchment area, for the average year and dry year, as shown in Figure 4, as a function of k, with K_c = 1.

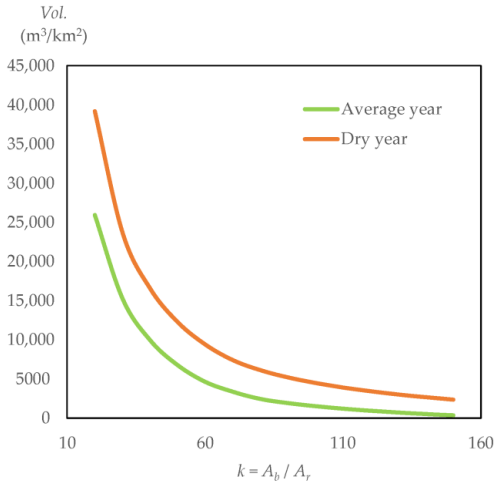

Figure 4. Curves of minimum usable reservoir volume per km^2 of upstream catchment area at the reservoir location for the average and dry years.

2.3.6. Reservoir Location Criteria

The selection of suitable sites for agricultural water reservoirs was supported by the automated computation of the water balance in a GIS environment for multiple points distributed along the watercourses, without identified buffer constraints. For each point, both the upstream catchment area contributing to surface runoff and the downstream irrigated area to be supplied were delineated.

Using Equations (6)–(9) and Figure 4, the minimum adequate storage volume of each potential reservoir was determined in GIS, corresponding to the minimum capacity required to allow complete filling and to meet irrigation demands during the summer months when the monthly hydrological balance becomes negative.

Among the stream segments presenting a positive hydrological balance, preference was given to locations situated closest and upstream to the agricultural polygons to be supplied, prioritising sites in natural recesses with steep slopes where the upstream section widens. These locations enable the formation of a sufficiently large water body for storage while minimising the embankment height. Field visits were subsequently conducted at the sites selected through this methodology to validate the locations that meet the proposed criteria (Figure 5).

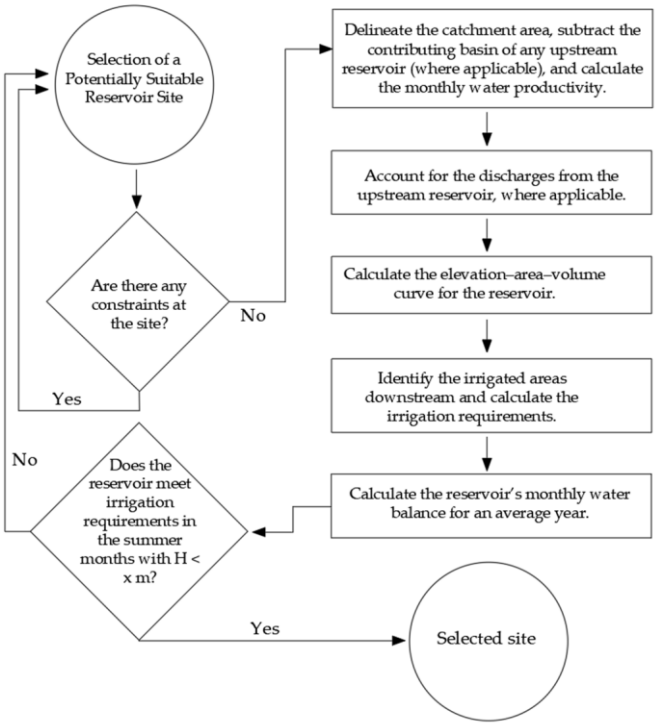

Figure 5. Methodology for Selecting Sites for the Construction of a New Reservoir.

Once an initial site has been selected, it may be appropriate to construct a second reservoir on the same watercourse downstream of the first to accommodate the discharges from the upstream reservoir and supply additional agricultural parcels. The decision criterion is shown in Figure 6.

To ensure the environmental and regulatory feasibility of the proposed reservoir sites, a spatial verification of constraints was conducted, focusing on Natura 2000 areas and land use regulations defined by the Municipal Master Plan (Plano Diretor Municipal) [26]. Official datasets from ICNF [27] were used to identify the boundaries of Natura 2000 sites. The analysis procedure confirmed which sites fall within, at the boundary of, or outside the protected area, providing the basis for subsequent site evaluation and decision making.

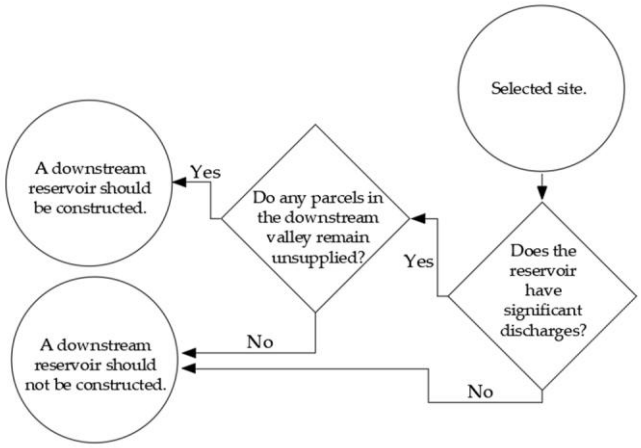

Figure 6. Decision criterion for constructing a second downstream reservoir.

3. Results

3.1. Identification of Irrigated Areas Based on NDVI

The mean NDVI across the four months was calculated for the municipality's agricultural zones and shown in Figure 7. The lowest values (<0.1) are the most frequent and presumably correspond to rainfed parcels. Conversely, the highest values (>0.4) are less common and represent areas of healthy, vigorous vegetation that may or may not be irrigated. Healthy trees and shrubs, even under rainfed conditions, strongly absorb red light and reflect strongly in the near-infrared region.

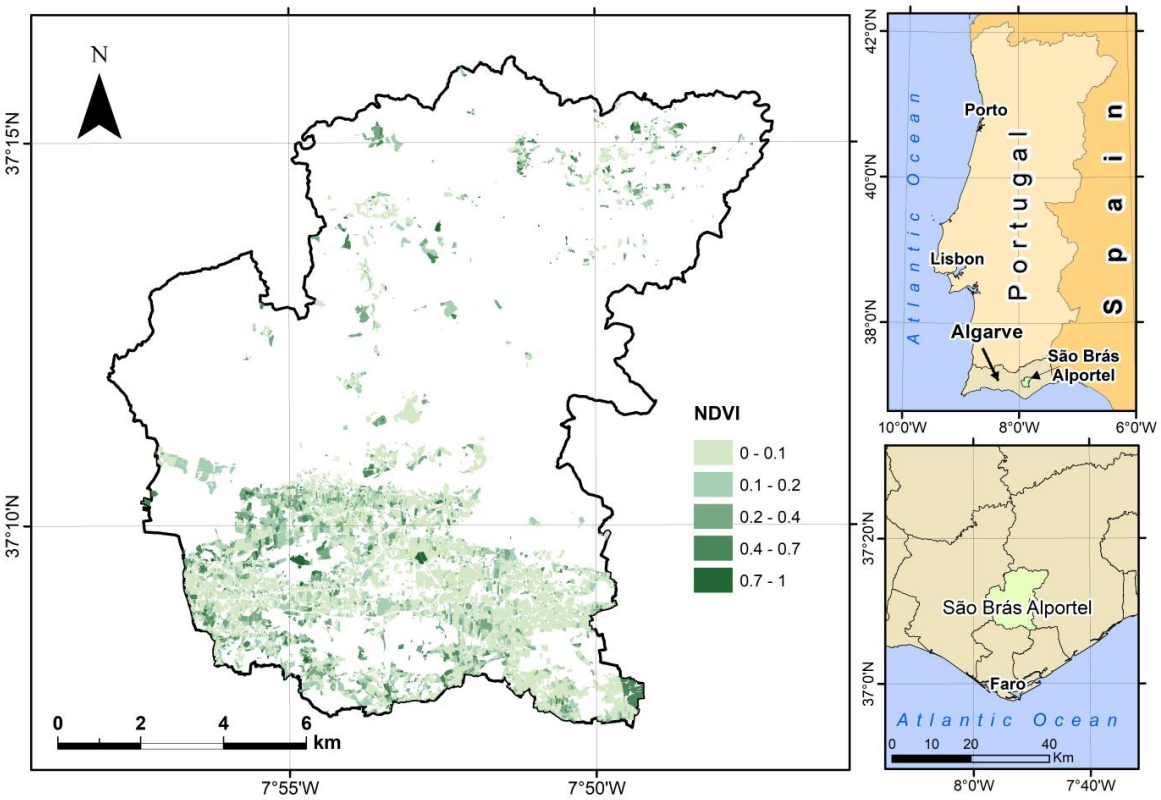

Figure 7. NDVI map.

3.2. Map of Irrigated and Rainfed Areas

Figure 8 delineates the irrigated and rainfed areas, considering parcels as irrigated if they contained at least 0.5 ha of pixels with NDVI values in the range of 0.40–0.71. The

total irrigated area identified using this criterion was 3 km^2, almost twice the area reported in official agricultural mapping, representing approximately 10% of the municipality's agricultural land.

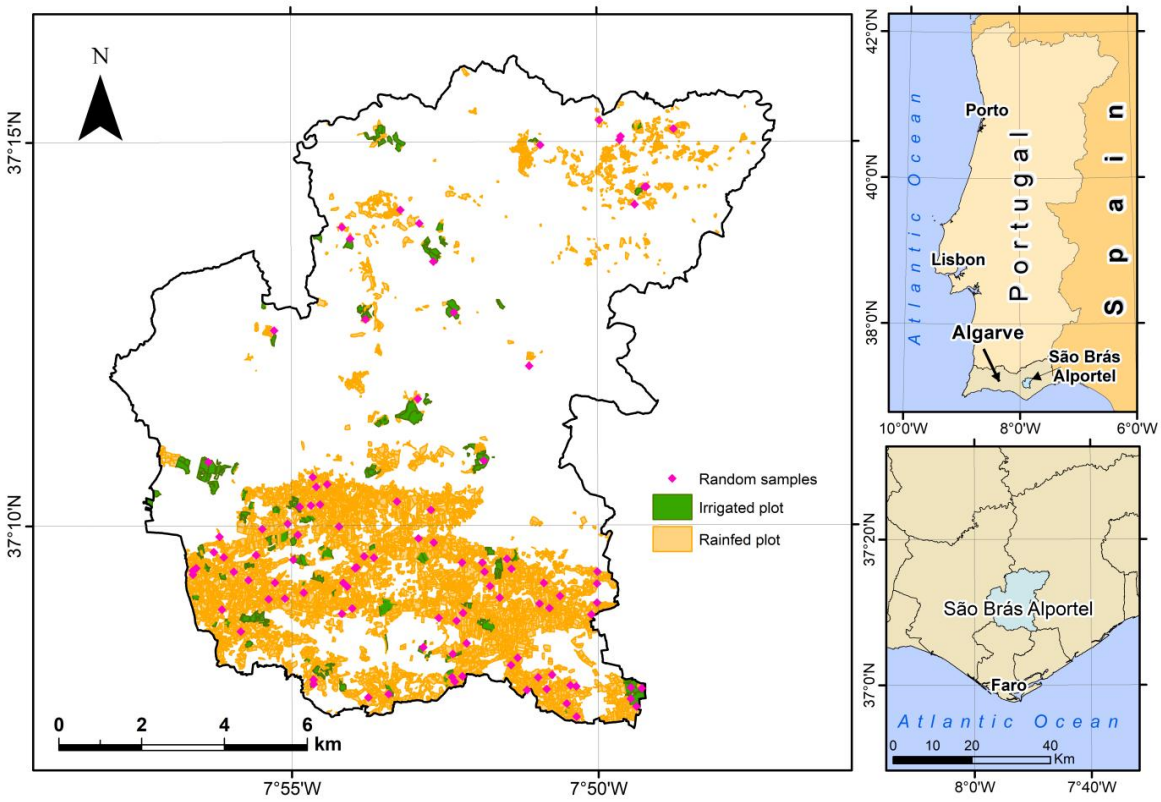

Figure 8. Map of Irrigated and Rainfed Areas.

The same map also plots the 100 randomly selected validation points to create the confusion matrix.

The confusion matrix employed to validate the delineation of irrigated and rainfed areas, shown in Figure 8, is presented in Table 7.

Table 7. Confusion Matrix.

Classified Areas	Reference Areas		Total
	Irrigated	Rainfed	
Irrigated	8	2	10
Rainfed	0	90	90
Total	8	92	100
Omission error, %	0.0	2.2	
Commission error, %	20.0	0.0	
User's accuracy, %	80.0	100.0	
Producer's accuracy, %	100	97.8	
Overall accuracy, %		98.0	
Kappa index, %		88.0	

As shown in Table 7, omission and commission errors were calculated for each class, corresponding to points that were not correctly identified and to false positives in the classification, respectively. For the irrigated class, the omission error was 0.0%, while the commission error reached 20.0%. Conversely, the omission error was 2.2% for the rainfed class, and the commission error was 0.0%. User's accuracy was 80.0% for the irrigated

class and 100% for the rainfed class, reflecting the reliability of the classification for each category. Producer's accuracy reached 100% for irrigated areas and 97.8% for rainfed areas, indicating the method's ability to identify each class correctly. Cohen's Kappa index was 0.88, which, on the Landis and Koch scale, represents almost perfect agreement [20]. Overall accuracy was 98%, with 98 of the 100 sampled points correctly classified, demonstrating the robustness of the agricultural area detection method.

The commission errors observed in the irrigated class are primarily associated with the presence of perennial rainfed crops and natural vegetation, which maintain relatively high photosynthetic activity during summer, resulting in NDVI values similar to those of irrigated areas. In São Brás de Alportel, these include olive groves (*Olea europaea*), almond trees (*Prunus dulcis*), fig trees (*Ficus carica*), and perennial shrub species such as *Cistus* spp., *Pistacia lentiscus*, *Quercus coccifera*, and *Rosmarinus officinalis*. Although these are rainfed systems, their structural and physiological adaptations to drought allow them to retain green biomass and relatively high vigour throughout the dry season, which explains the false positives and the resulting commission error observed for the irrigated class.

3.3. Creation of the Drainage Network from Digital Elevation Models

The resulting DEM, after sink correction, is shown in Figure 9. In the northern part of the study area, corresponding to the Serra do Caldeirão, elevations exceed 400 m, reaching a maximum of 528 m. By contrast, the southern sector is generally flatter, with broader valleys and elevations ranging from 120 to 350 m, making it more conducive to agricultural activity. Figure 10 illustrates the drainage network derived from flow-accumulation values exceeding 160 cells, with a total length of approximately 758 km. The associated micro-catchments are also indicated. In all, 38 micro-catchments were identified: in the upland zone, the Ribeira de Alportel and Ribeira das Mercês predominate, while in the Barrocal, the Ribeira de Gaifona is the principal stream.

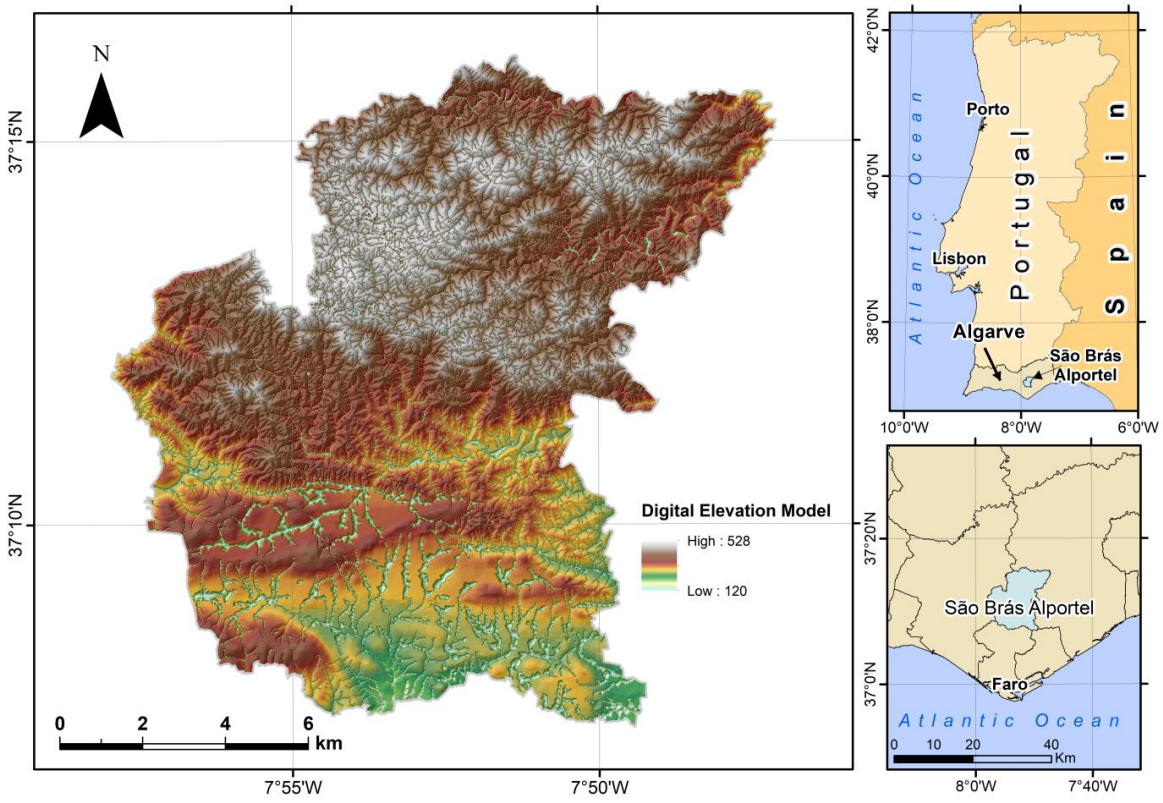

Figure 9. DEM of the Study Area.

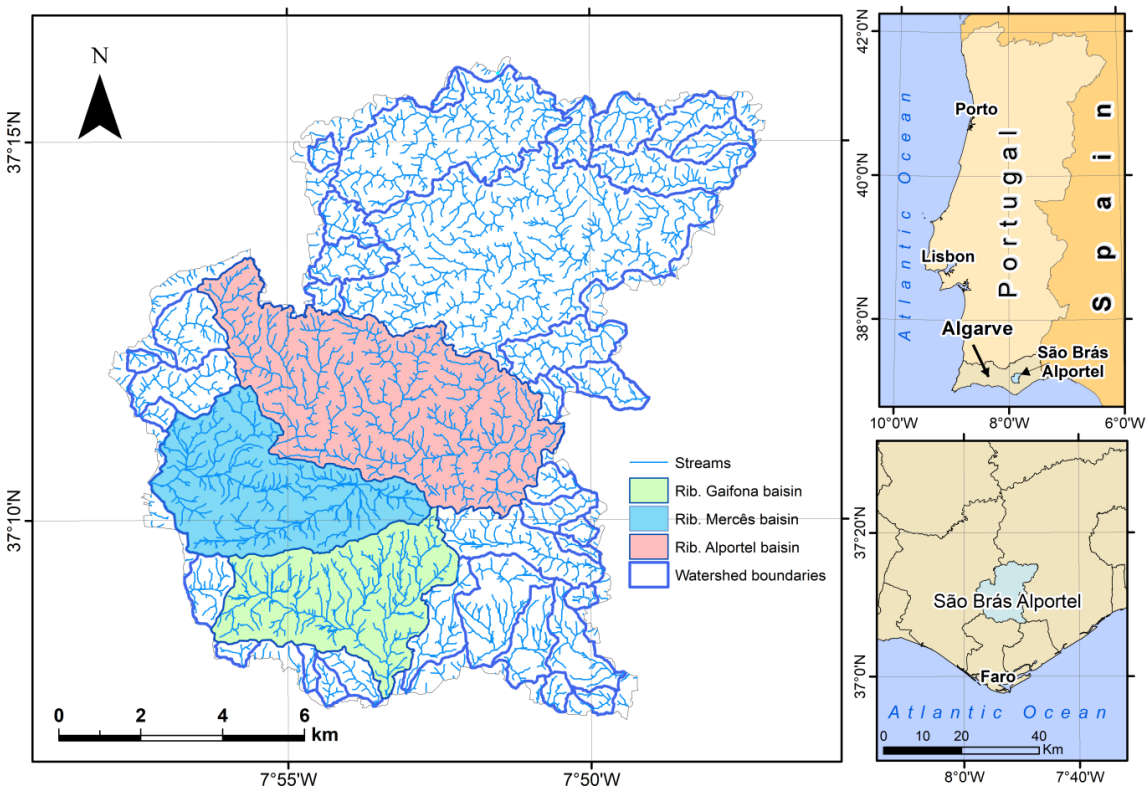

Figure 10. Drainage network and corresponding catchments for a flow-accumulation threshold of 160 cells.

Figure 11 shows the watercourses classified according to the Strahler method, in which order 1 represents the least significant streams and order 5 the most significant.

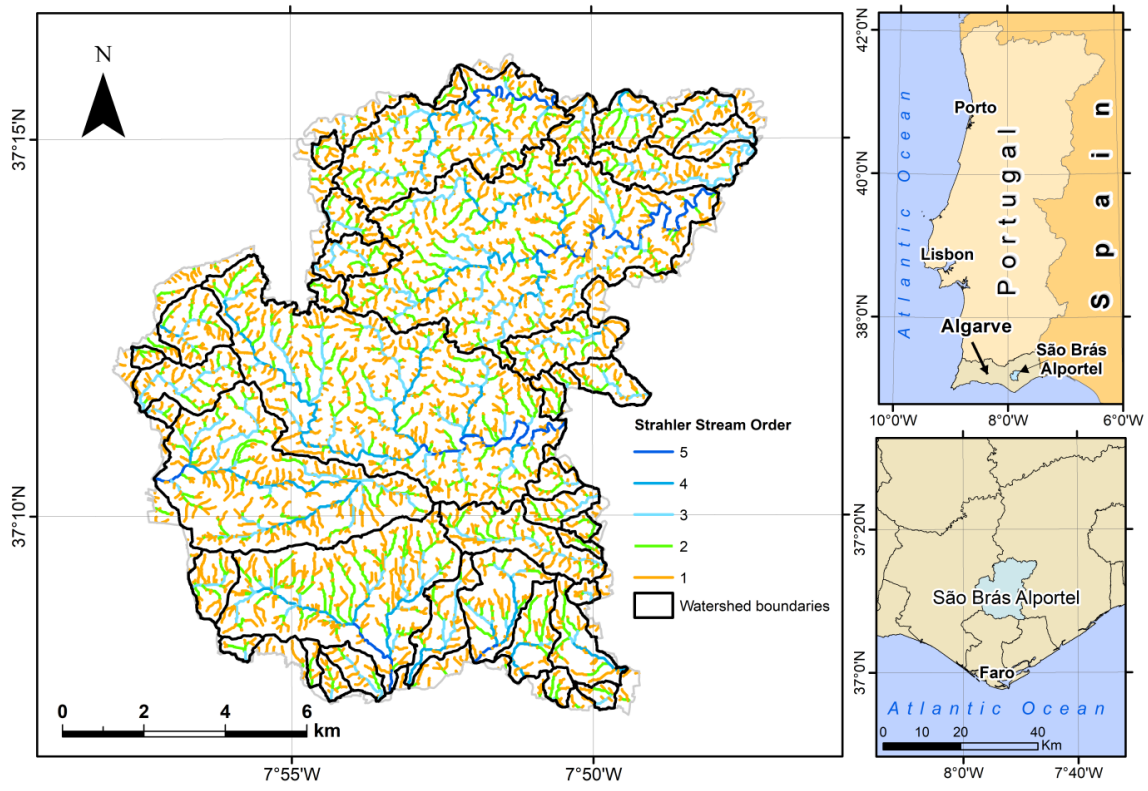

Figure 11. Stream network and corresponding catchments for a flow-accumulation threshold of 160 cells, classified according to the Strahler method.

Figure 12 displays the geometric network with downstream flow directions. This network represents the spatial and functional structure of the drainage system, enabling the identification of preferential surface runoff paths and facilitating the selection of the most suitable locations for reservoir construction.

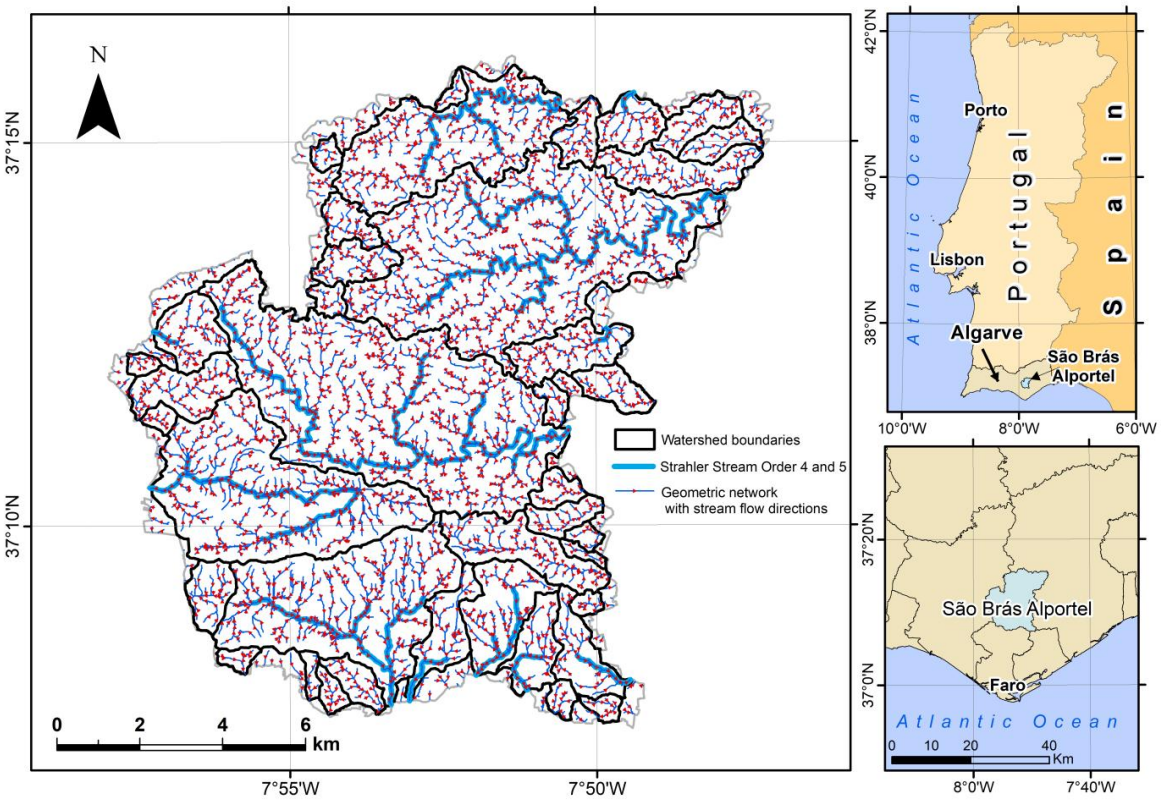

Figure 12. Map of downstream water-flow directions.

3.4. Selection of Sites for Reservoir Construction

Three strategic sites were selected, i.e., one on the Ribeira da Gaifona in the *Barrocal* zone, and two on the Ribeira das Mercês and the Ribeira de Alportel in the *Serra*.

A *Barrocal* location was chosen because most agricultural activity in the municipality is concentrated there; moreover, the municipal authority has undertaken to provide an impermeable reservoir floor at that site. The *Serra* sites were selected because their catchments are larger and lie closer to the Barrocal, where the municipality's main agricultural area is situated.

Specific dam sites were then pinpointed along each watercourse. The map of points that satisfy the reservoir-siting criteria is shown in Figure 13. Once the reservoir points had been fixed, the upstream catchments were delineated. The raster data were converted to vector format, and the drainage-basin area at each site was calculated. The outcome is depicted in the reservoir-catchment map in Figure 13.

The subsequent stage involved the systematic computation of the water balance in the GIS environment for multiple points along the watercourse.

For each point, both the upstream catchment area contributing to surface runoff and the downstream irrigated area to be supplied were determined.

Based on Equations (6) and (9) and Figure 6 presented in the methodological section, the minimum adequate storage volume of each reservoir was calculated, corresponding to the minimum volume required to ensure reservoir filling and to meet irrigation demands during the summer months, when the monthly water balance becomes negative.

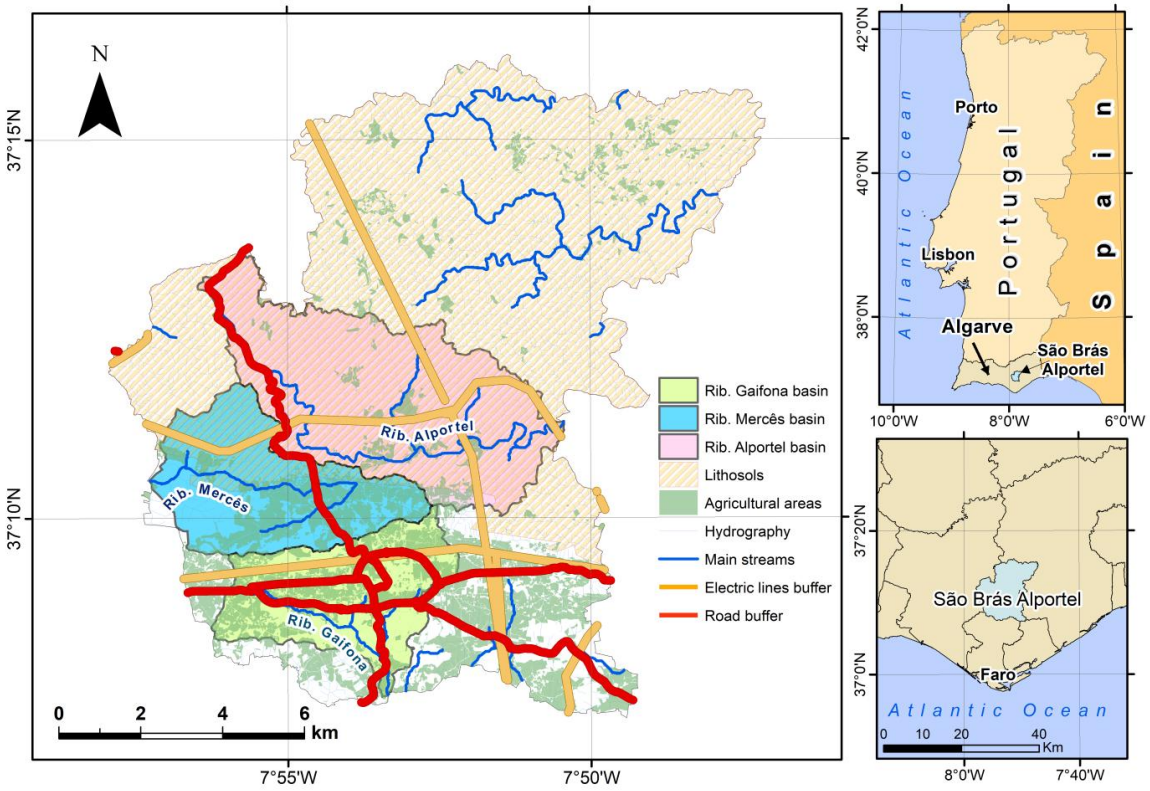

Figure 13. Overlay map showing catchment basins and watercourses together with roads and high-voltage power lines.

The systematic application of this procedure to the three streams under study resulted in the map shown in Figure 14.

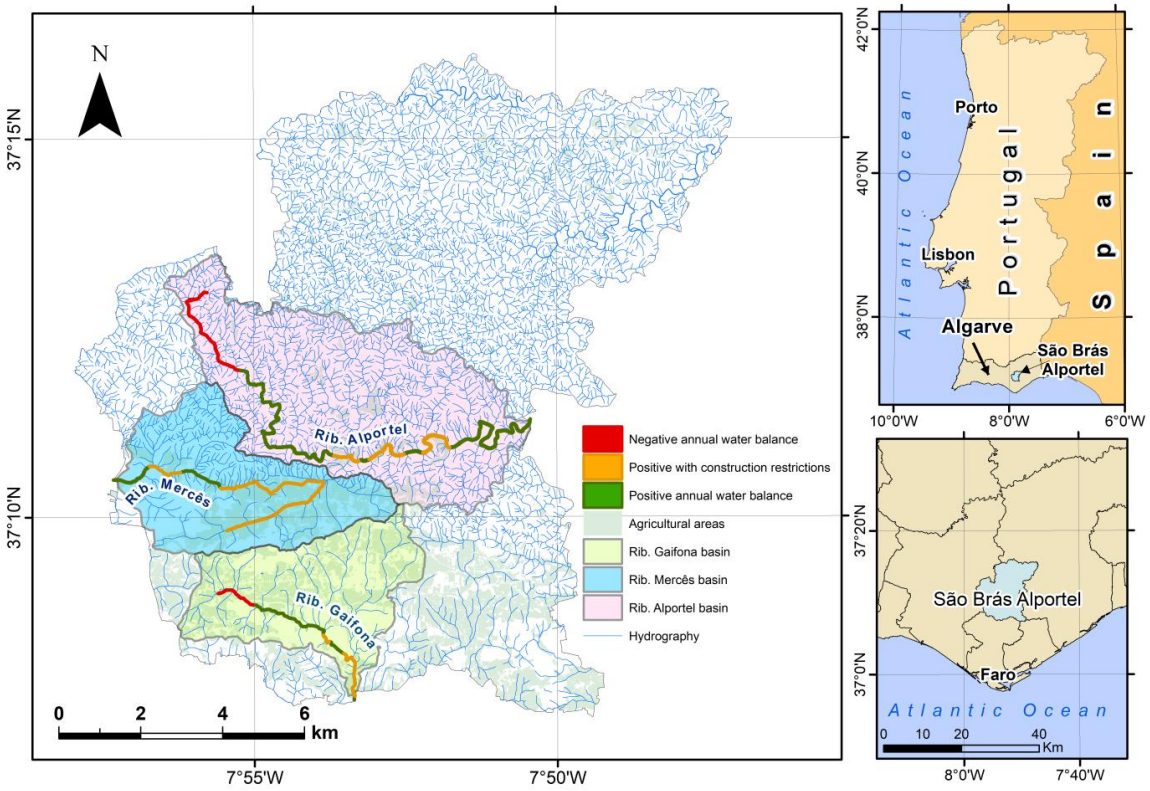

Figure 14. Overlay map showing watercourses and possible reservoir locations with positive (green), negative (red) annual water balance and positive (orange) with construction restrictions.

The red segments represent areas where the annual water balance is negative, meaning that the hydrological productivity of the upstream catchment is insufficient to meet the irrigation water demand of the downstream agricultural areas.

Conversely, the green segments identify locations where the annual water balance is positive, suggesting that it is possible to retain all or part of the runoff generated during the wetter months and to meet irrigation requirements throughout the dry season. Similarly, the orange zones denote areas of positive water balance; however, these areas are subject to construction restrictions.

The proposed reservoir sites on the Ribeira de Alportel and Ribeira das Mercês (corresponding to the green segments) are located in areas that overlap and partially coincide with the boundaries of two different Natura 2000 sites: Caldeirão (PTCON0057) and Barrocal (PTCON0049), respectively. Consequently, a detailed Appropriate Assessment will be required to ensure that no significant adverse effects occur on the protected habitats and species. Meanwhile, the proposed reservoir site on the Ribeira da Gaifona is located outside any Natura 2000 site or other legally protected area. However, part of the proposed site lies within a zone designated for natural protection and enhancement, according to information obtained from the São Brás de Alportel Municipal Master Plan (PDM), which should be duly considered in the environmental assessment.

Figure 15 shows the preferred locations along the Alportel, Mercês, and Gaifona streams for the construction of dam embankments. These sites are situated in narrow valleys with steep slopes, where the upstream section widens to accommodate the required storage volume while maintaining water depths between 8 m and 12 m. All selected reaches correspond to stream sections exhibiting a positive hydrological balance.

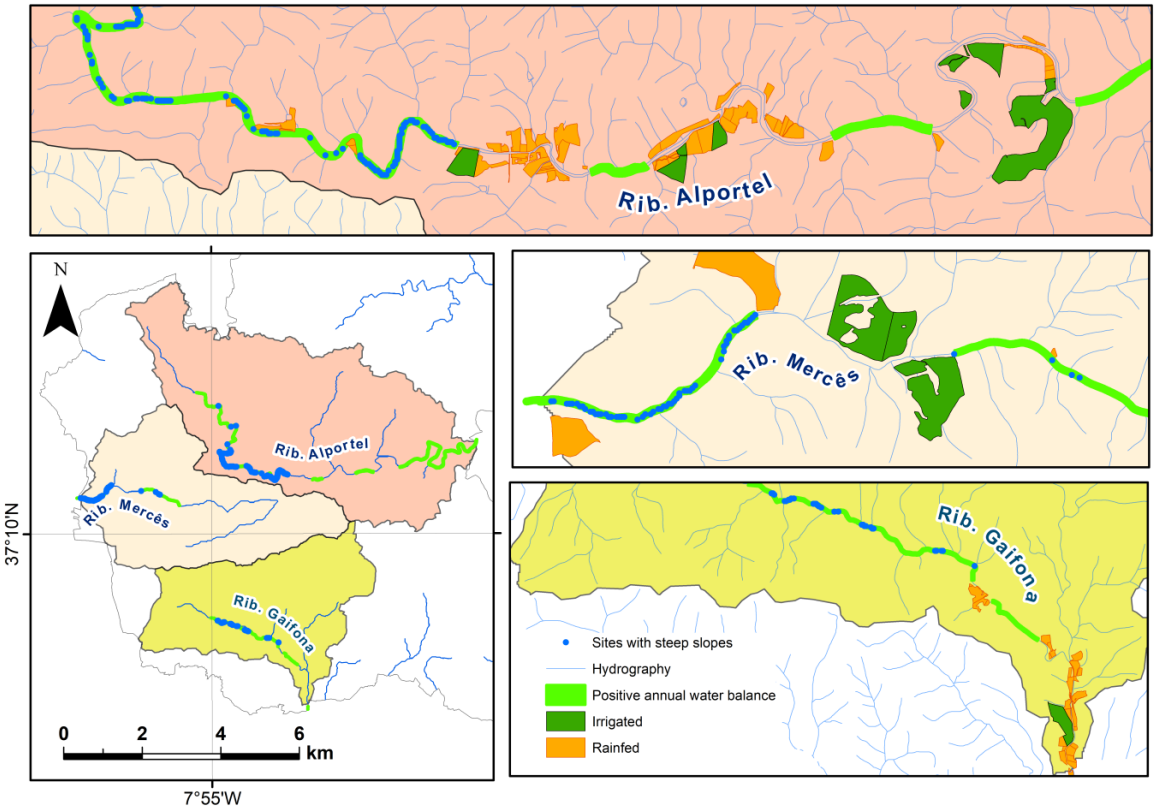

Figure 15. Preferred locations along the Alportel, Mercês, and Gaifona streams for the construction of dam embankments.

After applying the described methodology and conducting field visits, the suitable reservoir sites are presented in Figure 16. The figure shows the overlay of the

study area with the points selected for the reservoirs, including the upstream catchments and the rainfed and irrigated parcels downstream, providing a clear visualisation of the spatial distribution of the reservoirs in relation to the agricultural areas and the hydrological network.

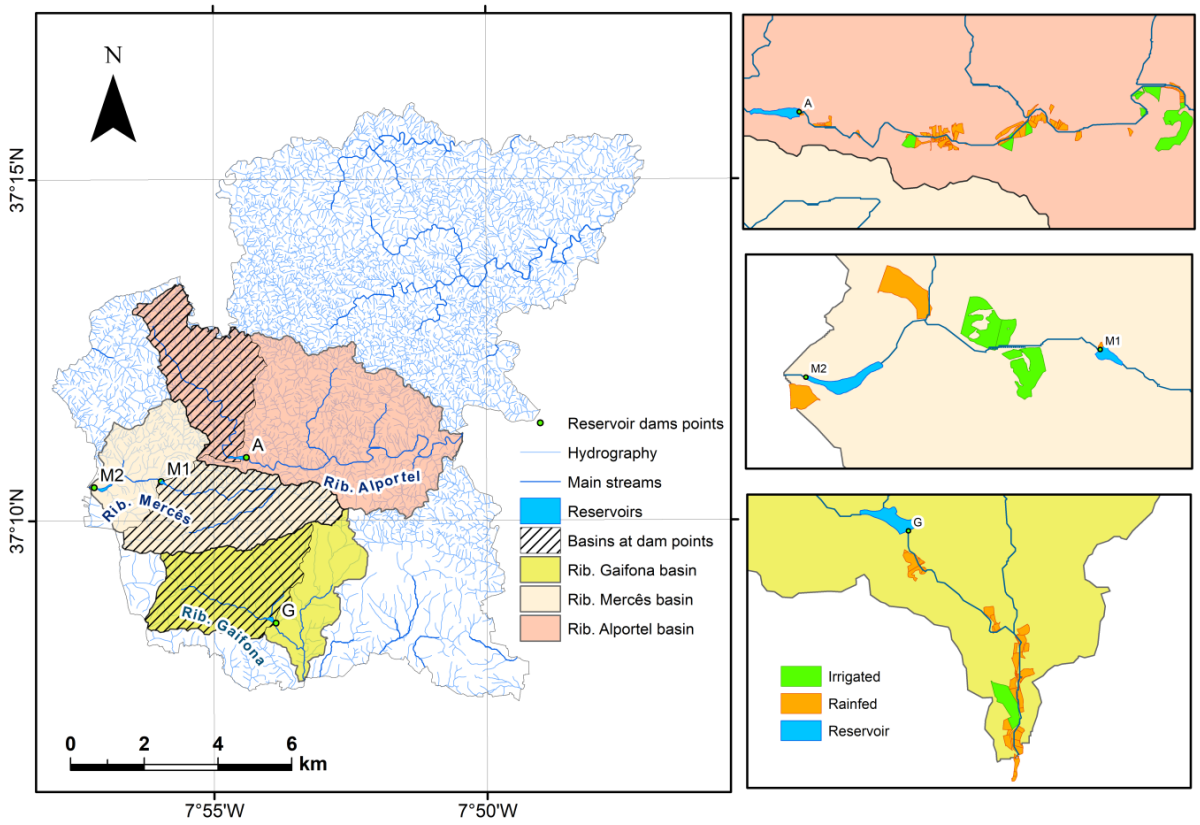

Figure 16. Location of the reservoirs in the Ribeiras of Alportel, Mercês, and Gaifona, and downstream the irrigated agricultural parcels (in green) and rainfed parcels (in orange).

The catchment areas and the upstream catchment areas at the reservoir dam sites are presented in Table 8.

Table 8. Catchment-area values and upstream catchment areas at the reservoir dam sites.

Catchment	Catchment Area (m^2)	Dam-Site Name	Catchment Area at the Dam Site (m^2)
Ribeira da Gaifona	14,115,200	G	8,656,758
Ribeira das Mercês	15,790,500	M1	9,598,495
Ribeira de Alportel	27,734,200	A	8,317,464

3.5. Reservoir Water-Balance Analysis

After the dam sites had been fixed, stage volume curves were produced for each reservoir. In this case study, embankments are to be limited to a maximum height of 12 m, with priority given to constructing several small reservoirs rather than one large structure.

The stage volume curves for the proposed reservoirs are presented in Figure 17.

At the current study stage, a maximum depth of 12 m, and less wherever feasible, has been assumed for all reservoirs, based on the existing topographic and geological conditions for water storage.

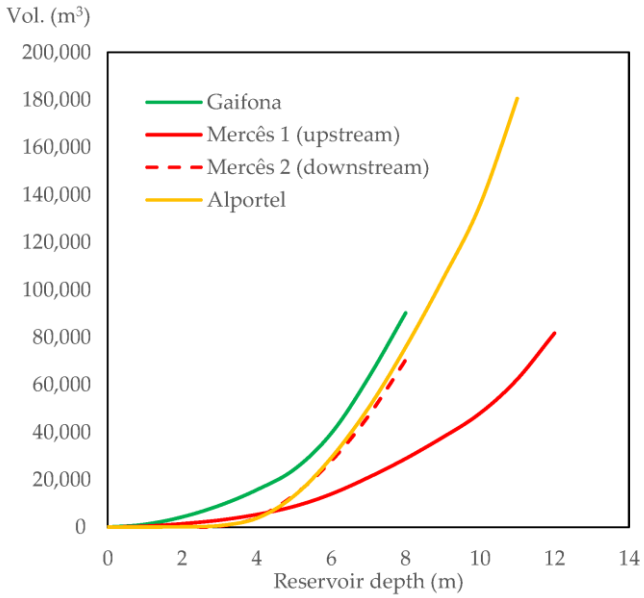

Figure 17. Stage–volume curves for the reservoirs.

3.6. Characterisation of the Agricultural Areas Served by the Reservoirs

For the four dam sites identified, the irrigated crop areas are listed in Table 9. The same table also specifies the minimum usable volumes and the total storage volumes adopted for the reservoirs.

Table 9. Crop areas supplied by the reservoirs, minimum usable volumes and total adopted volumes.

Crop	**Reservoir**			
	Gaifona	**Mercês 1**	**Mercês 2**	**Alportel**
Vineyard (m^2)	0	0	0	0
Vegetable garden (m^2)	107,140	0	0	605,800
Olive grove (m^2)	67,600	43,481	19,514	1,734,260
Orchard (m^2)	931,080	105,991	0	91,710
Ar (m^2)	1,105,820	149,472	19,514	2,431,770
Parameter	Reservoir			
	Gaifona	Mercês 1	Mercês 2	Alportel
Ab (km^2)	8.657	9.598	6.151	8.317
Ar (km^2)	0.1106	0.1495	0.1951	0.2560
Kc	0.71	0.66	0.61	0.72
$k = Ab/Ar$	78	64	315	32
Vol./km^2	2753	4238	1200	14,600
Reserv. Min. Vol. (m^3)	23,832	40,678	7381	121,435
Reserv. Vol. (m^3)	95,288	81,703	70,510	180,504

Olive groves and orchards are the predominant crops in the study area. Introducing irrigation increases productivity and makes agricultural activity economically viable.

3.7. Water Balance of the Reservoirs for the Average Year

Applying the methodology described above, Tables 10–13 present the water balance results in the average year for the Ribeiras da Gaifona, das Mercês, and de Alportel. The upstream catchment's water productivity in an average year enables the reservoir to fill rapidly. The monthly water balance begins in October, when stored water volumes are at their lowest, and ends in September, coinciding with the onset of the wet semester and the

start of the hydrological year. Only in June, July, August, and September does the balance become negative. Although stored volume falls during these months, it remains sufficient to meet irrigation demand throughout the summer.

For the Ribeira das Mercês, due to downstream irrigation needs, discharges through the spillway of the first reservoir, and valley conditions, a water balance analysis was conducted for secondary reservoirs located downstream, with the results presented in Table 13. In the downstream reservoir, as it receives discharges from the upstream reservoir, the monthly water balance is only negative in July and August.

The key water balance values in the average year for the four reservoirs are shown in Figure 18.

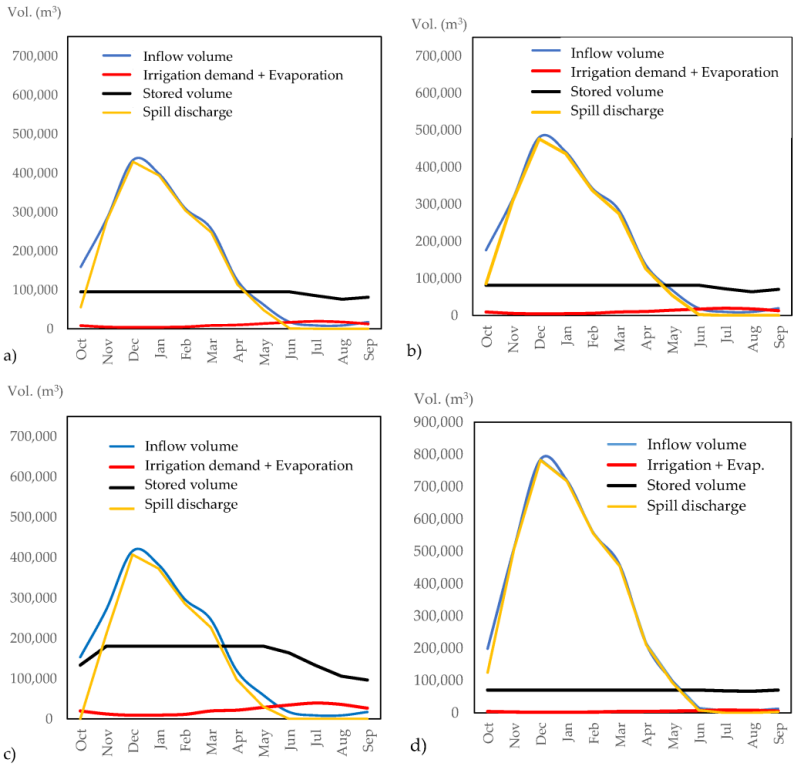

Figure 18. Monthly water balance values for the four reservoirs in the average year: (**a**) Gaifona; (**b**) Mercês 1 (upstream reservoir); (**c**) Alportel; (**d**) Mercês 2 (downstream reservoir).

Table 10. Water balance of the Ribeira da Gaifona for the average year.

(1)	(2)	(3)	(4)	(5)	(6)	(7)	(8)	(9)	(10)	(11)	(12)	(13)	(14)
										0	0	0	0
Oct	18.4	83	0.71	59	106.0	2144	6493	159,164	8637	150,527	150,527	95,288	55,238
Nov	32.7	49	0.71	35	61.6	1247	3866	282,958	5114	277,845	373,133	95,288	277,845
Dec	50.1	39	0.70	27	58.1	1176	3040	433,280	4216	429,064	524,352	95,288	429,064
Jan	46	43	0.75	32	45.8	927	3547	397,910	4473	393,437	488,725	95,288	393,437
Feb	35.8	52	0.75	39	57.3	1160	4289	309,486	5449	304,037	399,325	95,288	304,037
Mar	29.6	87	0.70	61	102.5	2075	6707	256,431	8782	247,649	342,937	95,288	247,649
Apr	14.3	100	0.70	70	113.3	2293	7776	123,794	10,069	113,725	209,014	95,288	113,725
May	7.15	137	0.69	95	149.1	3017	10,479	61,897	13,495	48,402	143,690	95,288	48,402
Jun	2.04	163	0.70	114	202.4	4097	12,608	17,685	16,705	980	96,268	95,288	980
Jul	1.02	185	0.69	128	257.5	5211	14,125	8842	19,336	−10,494	84,795	84,795	0
Aug	1.02	168	0.69	116	232.6	4707	12,827	8842	17,534	−8692	76,103	76,103	0
Sep	2.04	123	0.69	85	163.4	3306	9416	17,685	12,722	4963	81,066	81,066	0

(1) Month; (2) Runoff * (mm); (3) ETo ** (mm); (4) Kc; (5) ETc (mm); (6) Pan evaporation *** (mm); (7) Reservoir evaporation (m^3); (8) Irrigation demand (m^3); (9) Inflow volume (m^3); (10) Outflow volume (m^3); (11) ΔV (m^3); (12) Balance (m^3); (13) Stored volume (m^3); (14) Spill discharge (m^3); * Mean monthly runoff—RH8, Arade catchment [22]; ** Mean monthly evapotranspiration—São Bartolomeu de Messines, 2006–2022 [28]; *** Monthly pan evaporation—São Brás de Alportel [24].

Table 11. Water balance of the Ribeira das Mercês (upstream reservoir) for the average year.

(1)	(2)	(3)	(4)	(5)	(6)	(7)	(8)	(9)	(10)	(11)	(12)	(13)	(14)
										0	0	0	0
Oct	1.0	83	0.67	56	106	912	8348	9804	9261	544	544	544	0
Nov	3.1	49	0.70	34	62	531	5142	29,413	5672	23,741	24,285	24,285	0
Dec	5.1	39	0.66	26	58	500	3855	49,022	4355	44,667	68,951	68,951	0
Jan	6.1	43	0.69	30	46	394	4441	58,826	4835	53,991	122,943	81,703	41,239
Feb	6.1	52	0.69	36	57	494	5370	58,826	5864	52,963	134,666	81,703	52,963
Mar	4.1	87	0.66	57	103	883	8545	39,218	9428	29,790	111,493	81,703	29,790
Apr	4.1	100	0.65	65	113	976	9754	39,218	10,729	28,488	110,192	81,703	28,488
May	2.0	137	0.63	86	149	1284	12,920	19,609	14,203	5406	87,109	81,703	5406
Jun	1.0	163	0.64	104	202	1743	15,473	9804	17,216	−7412	74,291	74,291	0
Jul	0.5	185	0.63	116	258	2217	17,285	4902	19,502	−14,600	59,691	59,691	0
Aug	0.2	168	0.63	105	233	2003	15,697	1961	17,700	−15,739	43,952	43,952	0
Sep	0.2	123	0.63	78	163	1407	11,653	1920	13,059	−11,140	32,813	32,813	0

(1) Month; (2) Runoff * (mm); (3) ETo ** (mm); (4) Kc; (5) ETc (mm); (6) Pan evaporation *** (mm); (7) Reservoir evaporation (m^3); (8) Irrigation demand (m^3); (9) Inflow volume (m^3); (10) Outflow volume (m^3); (11) ΔV (m^3); (12) Balance (m^3); (13) Stored volume (m^3); (14) Spill discharge (m^3); * Mean monthly runoff—RH8, Arade catchment [22]; ** Mean monthly evapotranspiration—São Bartolomeu de Messines, 2006–2022 [28]; *** Monthly pan evaporation—São Brás de Alportel [24].

Table 12. Water balance of the Ribeira do Alportel for the average year.

(1)	(2)	(3)	(4)	(5)	(6)	(7)	(8)	(9)	(10)	(11)	(12)	(13)	(14)
										0	0	0	0
Oct	18.4	83	0.77	64	106	3002	16,400	152,926	19,402	133,524	133,524	133,524	0
Nov	32.7	49	0.84	41	62	1746	10,577	271,868	12,323	259,545	393,069	180,504	212,565
Dec	50.1	39	0.74	29	58	1646	7421	416,298	9067	407,231	587,735	180,504	407,231
Jan	46.0	43	0.73	31	46	1297	8046	382,314	9343	372,971	553,475	180,504	372,971
Feb	35.8	52	0.73	38	57	1624	9730	297,356	11,354	286,002	466,506	180,504	286,002
Mar	29.6	87	0.75	65	103	2905	16,705	246,380	19,610	226,770	407,274	180,504	226,770
Apr	14.3	100	0.72	72	113	3210	18,481	118,942	21,691	97,251	277,755	180,504	97,251
May	7.2	137	0.69	94	149	4223	24,055	59,471	28,278	31,193	211,697	180,504	31,193
Jun	2.0	163	0.68	111	202	5735	28,338	16,992	34,073	−17,081	163,423	163,423	0
Jul	1.0	185	0.67	124	258	7294	31,808	8496	39,102	−30,606	132,817	132,817	0
Aug	1.0	168	0.67	113	233	6589	28,885	8496	35,474	−26,978	105,839	105,839	0
Sep	2.0	123	0.69	85	163	4628	21,821	16,992	26,449	−9457	96,381	96,381	0

(1) Month; (2) Runoff * (mm); (3) ETo ** (mm); (4) Kc; (5) ETc (mm); (6) Pan evaporation *** (mm); (7) Reservoir evaporation (m^3); (8) Irrigation demand (m^3); (9) Inflow volume (m^3); (10) Outflow volume (m^3); (11) ΔV (m^3); (12) Balance (m^3); (13) Stored volume (m^3); (14) Spill discharge (m^3); * Mean monthly runoff—RH8, Arade catchment [22]; ** Mean monthly evapotranspiration—São Bartolomeu de Messines, 2006–2022 [28]; *** Monthly pan evaporation—São Brás de Alportel [24].

Table 13. Water balance of the Ribeira das Mercês (downstream reservoir) for the average year.

(1)	(2)	(3)	(4)	(5)	(6)	(7)	(8)	(9)	(10)	(11)	(12)	(13)	(14)	(15)
											0	0	0	0
Oct	18.4	83	0.68	56	85,515	106.0	2749	1101	198,606	3850	194,755	194,755	70,510	124,245
Nov	32.7	49	0.78	38	308,068	61.6	1599	746	509,119	2345	506,774	577,284	70,510	506,774
Dec	50.1	39	0.64	25	476,060	58.1	1508	487	783,918	1995	781,924	852,434	70,510	781,924
Jan	46	43	0.62	27	436,362	45.8	1188	520	719,089	1708	717,381	787,891	70,510	717,381
Feb	35.8	52	0.62	32	337,290	57.3	1487	629	557,189	2116	555,073	625,583	70,510	555,073
Mar	29.6	87	0.65	57	274,899	102.5	2660	1104	457,101	3764	453,338	523,848	70,510	453,338
Apr	14.3	100	0.61	61	126,532	113.3	2940	1190	214,491	4130	210,361	280,871	70,510	210,361
May	7.15	137	0.56	77	54,428	149.1	3867	1497	98,407	5365	93,043	163,553	70,510	93,043
Jun	2.04	163	0.55	90	2392	202.4	5252	1749	14,958	7001	7957	78,467	70,510	7957
Jul	1.02	185	0.54	100	0	257.5	6680	1949	6283	8630	−2347	68,163	68,163	0
Aug	1.02	168	0.54	91	0	232.6	6035	1770	6283	7805	−1522	66,641	66,641	0
Sep	2.04	123	0.57	70	0	163.4	4238	1368	12,566	5606	6959	73,600	70,510	3090

(1) Month; (2) Runoff * (mm); (3) ETo ** (mm); (4) Kc; (5) ETc (mm); (6) Reservoir 1 spill discharge (m^3); (7) Pan evaporation *** (mm); (8) Reservoir 2 evaporation (m^3); (9) Irrigation demand (m^3); (10) Inflow to reservoir 2 (m^3); (11) Outflow from reservoir 2 (m^3); (12) ΔV in reservoir 2 (m^3); (13) Balance in reservoir 2 (m^3); (14) Stored volume in reservoir 2 (m^3); (15) Reservoir 2 spill discharge (m^3); * Mean monthly runoff—RH8, Arade catchment [22]; ** Mean monthly evapotranspiration—São Bartolomeu de Messines, 2006–2022 [28]; *** Monthly pan evaporation—São Brás de Alportel [24].

The stored volume and spill discharge curves for the four reservoirs are shown in Figure 19.

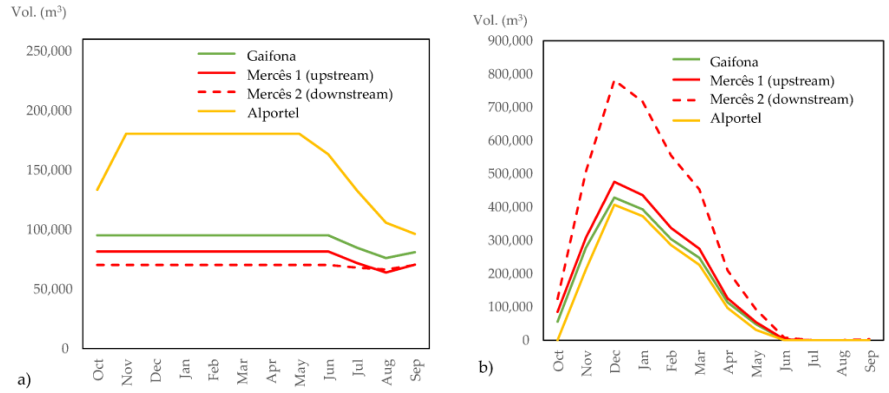

Figure 19. Key results from the monthly hydrological balance for the four reservoirs in the average year: (**a**) Stored volume curves for the reservoirs and (**b**) Reservoir spill discharges.

The monthly hydrological balance in the average year indicates that the reservoirs fill readily, with a positive balance for almost the entire year, except in June, July, August, and, in some cases, September. During these summer months, the balance turns negative; yet, the stored volume still suffices to maintain irrigation demand and compensate for direct evaporation. The analysis further reveals that runoff in the first two months of the hydrological year (October and November) is adequate to refill all the reservoirs; whenever the cumulative monthly inflow exceeds capacity, surplus water is discharged to the stream and continues along its natural course to the sea.

Runoff from the upstream catchments is thus high in an average year, and the reservoirs spill from October to May. Even under these conditions, the irrigated area remains relatively small compared with the region's water potential: the total capacities of the reservoirs considered are two to three times greater than the minimum usable volumes required to meet irrigation demand in summer.

Constructing two reservoirs in series on the same watercourse, a cascade, offers the advantage of replacing a single, larger structure with several smaller reservoirs distributed along the watercourse. Besides being the most obvious solution, this arrangement stores more water for agriculture and other uses closer to the points of demand, reducing both landscape and environmental impact.

3.8. Water Balance of the Reservoirs for the Dry Year

Applying the same methodology described above, Tables 14–16 present the water balance results in the dry year for the Ribeiras da Gaifona, das Mercês, and de Alportel. The monthly water balance begins in October, when stored water volumes are at their lowest, and ends in September, coinciding with the onset of the wet season and the start of the hydrological year. The upstream catchment's water productivity in a dry year still enables the reservoir to fill from October, when the rainy season starts, to January. Only in June, July, August, and September does the balance become negative. Although stored volume falls during these months, it remains sufficient to meet irrigation demand and compensate for the evaporation throughout the summer.

In the dry year, Ribeira Mercês upstream reservoir continues to have discharges through the spillway from January to May, justifying the existence of a second downstream reservoir. In the downstream reservoir, as it receives discharges from the upstream reservoir, the monthly water balance becomes negative in June, July, August, and September during dry years (Table 17).

Table 14. Water balance of the Ribeira da Gaifona reservoir for the dry year.

(1)	(2)	(3)	(4)	(5)	(6)	(7)	(8)	(9)	(10)	(11)	(12)	(13)	(14)
										0	0	0	0
Oct	1.0	83	0.71	59	106.0	2144	6493	8842	8637	205	205	205	0
Nov	3.1	49	0.71	35	61.6	1247	3866	26,527	5114	21,414	21,619	21,619	0
Dec	5.1	39	0.70	27	58.1	1176	3040	44,212	4216	39,996	61,615	61,615	0
Jan	6.1	43	0.75	32	45.8	927	3547	53,055	4473	48,581	110,196	95,288	14,908
Feb	6.1	52	0.75	39	57.3	1160	4289	53,055	5449	47,606	142,894	95,288	47,606
Mar	4.1	87	0.70	61	102.5	2075	6707	35,370	8782	26,587	121,876	95,288	26,587
Apr	4.1	100	0.70	70	113.3	2293	7776	35,370	10,069	25,301	120,589	95,288	25,301
May	2.0	137	0.69	95	149.1	3017	10,479	17,685	13,495	4189	99,478	95,288	4189
Jun	1.0	163	0.70	114	202.4	4097	12,608	8842	16,705	−7862	87,426	87,426	0
Jul	0.5	185	0.69	128	257.5	5211	14,125	4421	19,336	−14,915	72,511	72,511	0
Aug	0.2	168	0.69	116	232.6	4707	12,827	1768	17,534	−15,766	56,745	56,745	0
Sep	0.2	123	0.69	85	163.4	3306	9416	1731	12,722	−10,991	45,755	45,755	0

(1) Month; (2) Runoff * (mm); (3) ETo ** (mm); (4) Kc; (5) ETc (mm); (6) Pan evaporation *** (mm); (7) Reservoir evaporation (m^3); (8) Irrigation demand (m^3); (9) Inflow volume (m^3); (10) Outflow volume (m^3); (11) ΔV (m^3); (12) Balance (m^3); (13) Stored volume (m^3); (14) Spill discharge (m^3); * Mean monthly runoff—RH8, Arade catchment [22]; ** Mean monthly evapotranspiration—São Bartolomeu de Messines, 2006–2022 [28]; *** Monthly pan evaporation—São Brás de Alportel [24].

Table 15. Water balance of the Ribeira das Mercês upstream reservoir for the dry year.

(1)	(2)	(3)	(4)	(5)	(6)	(7)	(8)	(9)	(10)	(11)	(12)	(13)	(14)
										0	0	0	0
Oct	1.0	83	0.67	56	106	912	8348	9804	9261	544	544	544	0
Nov	3.1	49	0.70	34	62	531	5142	29,413	5672	23,741	24,285	24,285	0
Dec	5.1	39	0.66	26	58	500	3855	49,022	4355	44,667	68,951	68,951	0
Jan	6.1	43	0.69	30	46	394	4441	58,826	4835	53,991	122,943	81,703	41,239
Feb	6.1	52	0.69	36	57	494	5370	58,826	5864	52,963	134,666	81,703	52,963
Mar	4.1	87	0.66	57	103	883	8545	39,218	9428	29,790	111,493	81,703	29,790
Apr	4.1	100	0.65	65	113	976	9754	39,218	10,729	28,488	110,192	81,703	28,488
May	2.0	137	0.63	86	149	1284	12,920	19,609	14,203	5406	87,109	81,703	5406
Jun	1.0	163	0.64	104	202	1743	15,473	9804	17,216	−7412	74,291	74,291	0
Jul	0.5	185	0.63	116	258	2217	17,285	4902	19,502	−14,600	59,691	59,691	0
Aug	0.2	168	0.63	105	233	2003	15,697	1961	17,700	−15,739	43,952	43,952	0
Sep	0.2	123	0.63	78	163	1407	11,653	1920	13,059	−11,140	32,813	32,813	0

(1) Month; (2) Runoff * (mm); (3) ETo ** (mm); (4) Kc; (5) ETc (mm); (6) Pan evaporation *** (mm); (7) Reservoir evaporation (m^3); (8) Irrigation demand (m^3); (9) Inflow volume (m^3); (10) Outflow volume (m^3); (11) ΔV (m^3); (12) Balance (m^3); (13) Stored volume (m^3); (14) Spill discharge (m^3); * Mean monthly runoff—RH8, Arade catchment [22]; ** Mean monthly evapotranspiration—São Bartolomeu de Messines, 2006–2022 [28]; *** Monthly pan evaporation—São Brás de Alportel [24].

Table 16. Water balance of the Ribeira do Alportel reservoir for the dry year.

(1)	(2)	(3)	(4)	(5)	(6)	(7)	(8)	(9)	(10)	(11)	(12)	(13)	(14)
										0	0	0	0
Oct	1.0	83	0.77	64	106	3002	16,400	8496	19,402	−10,906	−10,906	0	0
Nov	3.1	49	0.84	41	62	1746	10,577	25,488	12,323	13,165	13,165	13,165	0
Dec	5.1	39	0.74	29	58	1646	7421	42,479	9067	33,412	46,577	46,577	0
Jan	6.1	43	0.73	31	46	1297	8046	50,975	9343	41,632	88,209	88,209	0
Feb	6.1	52	0.73	38	57	1624	9730	50,975	11,354	39,621	127,830	127,830	0
Mar	4.1	87	0.75	65	103	2905	16,705	33,984	19,610	14,373	142,203	142,203	0
Apr	4.1	100	0.72	72	113	3210	18,481	33,984	21,691	12,292	154,496	154,496	0
May	2.0	137	0.69	94	149	4223	24,055	16,992	28,278	−11,286	143,209	143,209	0
Jun	1.0	163	0.68	111	202	5735	28,338	8496	34,073	−25,577	117,632	117,632	0
Jul	0.5	185	0.67	124	258	7294	31,808	4248	39,102	−34,854	82,778	82,778	0
Aug	0.2	168	0.67	113	233	6589	28,885	1699	35,474	−33,775	49,003	49,003	0
Sep	0.2	123	0.69	85	163	4628	21,821	1663	26,449	−24,786	24,217	24,217	0

(1) Month; (2) Runoff * (mm); (3) ETo ** (mm); (4) Kc; (5) ETc (mm); (6) Pan evaporation *** (mm); (7) Reservoir evaporation (m^3); (8) Irrigation demand (m^3); (9) Inflow volume (m^3); (10) Outflow volume (m^3); (11) ΔV (m^3); (12) Balance (m^3); (13) Stored volume (m^3); (14) Spill discharge (m^3); * Mean monthly runoff—RH8, Arade catchment [22]; ** Mean monthly evapotranspiration—São Bartolomeu de Messines, 2006–2022 [28]; *** Monthly pan evaporation—São Brás de Alportel [24].

Table 17. Water balance of the Ribeira das Mercês downstream reservoir for the dry year.

(1)	(2)	(3)	(4)	(5)	(6)	(7)	(8)	(9)	(10)	(11)	(12)	(13)	(14)	(15)
											0	0	0	0
Oct	1.02	83	0.68	56	0	106.0	2749	1101	6283	3850	2432	2432	2432	0
Nov	3.06	49	0.78	38	0	61.6	1599	746	18,848	2345	16,504	18,936	18,936	0
Dec	5.11	39	0.64	25	41,239	58.1	1508	487	72,653	1995	70,659	89,595	70,510	19,085
Jan	6.13	43	0.62	27	52,963	45.8	1188	520	90,660	1708	88,951	159,461	70,510	88,951
Feb	6.13	52	0.62	32	29,790	57.3	1487	629	67,487	2116	65,371	135,881	70,510	65,371
Mar	4.09	87	0.65	57	28,488	102.5	2660	1104	53,619	3764	49,856	120,366	70,510	49,856
Apr	4.09	100	0.61	61	5406	113.3	2940	1190	30,537	4130	26,407	96,917	70,510	26,407
May	2.04	137	0.56	77	0	149.1	3867	1497	12,566	5365	7201	77,711	70,510	7201
Jun	1.02	163	0.55	90	0	202.4	5252	1749	6283	7001	−718	69,792	69,792	0
Jul	0.51	185	0.54	100	0	257.5	6680	1949	3141	8630	−5488	64,303	64,303	0
Aug	0.2	168	0.54	91	0	232.6	6035	1770	1257	7805	−6548	57,755	57,755	0
Sep	0.2	123	0.57	70	0	163.4	4238	1368	1230	5606	−4376	53,379	53,379	0

(1) Month; (2) Runoff * (mm); (3) ETo ** (mm); (4) Kc; (5) ETc (mm); (6) Reservoir 1 spill discharge (m^3); (7) Pan evaporation *** (mm); (8) Reservoir 2 evaporation (m^3); (9) Irrigation demand (m^3); (10) Inflow to reservoir 2 (m^3); (11) Outflow from reservoir 2 (m^3); (12) ΔV in reservoir 2 (m^3); (13) Balance in reservoir 2 (m^3); (14) Stored volume in reservoir 2 (m^3); (15) Reservoir 2 spill discharge (m^3); * Mean monthly runoff—RH8, Arade catchment [22]; ** Mean monthly evapotranspiration—São Bartolomeu de Messines, 2006–2022 [28]; *** Monthly pan evaporation—São Brás de Alportel [24].

The key water balance values for the four reservoirs during the dry year are shown in Figure 20.

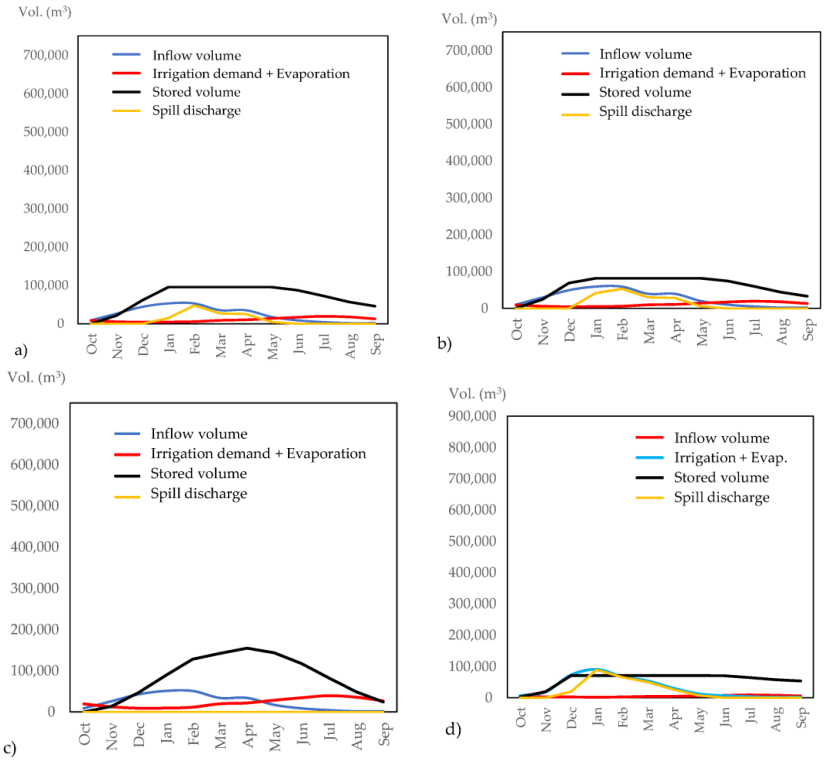

Figure 20. Monthly water balance values for the four reservoirs in the dry year: (**a**) Gaifona; (**b**) Mercês 1 (upstream reservoir); (**c**) Alportel; (**d**) Mercês 2 (downstream reservoir).

The stored volume and spill discharge curves for the four reservoirs in the dry year are shown in Figure 21.

During the dry year, the monthly hydrological balance indicates that all reservoirs continue to fill, showing a positive balance for most of the year, except during June, July, August, September, and October, when the balance becomes negative. However, while most reservoirs reach full capacity, the Alportel reservoir does not; yet it still provides sufficient storage to meet water demand throughout the year. Despite the seasonal deficit, the stored volume in the system remains adequate to sustain irrigation needs and compensate for

direct evaporation. The analysis further reveals that, in dry years, spill discharges decrease substantially and become residual compared to the average year.

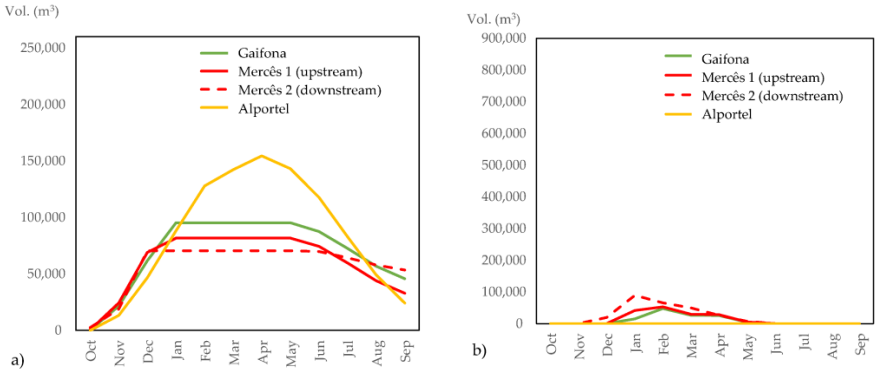

Figure 21. Key results from the monthly hydrological balance for the four reservoirs in the dry year: (**a**) Stored volume curves for the reservoirs and (**b**) Reservoir spill discharges.

4. Discussion of the Results

The discussion centres on three principal axes: spatial characterisation of irrigation, annual water availability and structural constraints. The high reliability of the irrigation map produced from NDVI (overall accuracy = 98%; K = 88%) confirms the potential of the low-complexity remote sensing approach adopted here. Comparable results (88–92% accuracy) were reported by [29] when identifying irrigated orchards on the Spanish Meseta using combined Sentinel-1 and Sentinel-2 time series, which reinforces the robustness of this type of classification in highly heterogeneous Mediterranean settings.

In an average-rainfall year, the São Brás reservoirs fill between the first two months of the rainy season, October and November. The monthly water balance turns negative only from July to September; yet, stored volumes remain sufficient for irrigation, keeping the annual cumulative balance positive.

In a dry year, the reservoirs take four months to fill, from October when the rainy season starts to January. Only in June, July, August, and September does the balance become negative. Although stored volume falls during these months, it also remains sufficient to meet irrigation demand and compensate for evaporation throughout the summer. Evaporation losses, estimated from SNIRH records (45.8–257.6 mm month^{-1}), lie within the range reported for large Mediterranean reservoirs [30]. Recent literature, however, warns that a +2 °C thermal increase could raise these losses by 15–20% [31], a reduction that should be taken into account in future sizing. These findings indicate refill ratios of more than 80% in the first two hydrological months, consistent with other Mediterranean studies, which describe 70–80% of annual runoff occurring in the wet half-year [32].

Najran's modelling shows a similar seasonal concentration, with the nine proposed ponds storing a combined 3.45 Mm^3 from catchments ranging from 40 to 212 km^2 and releasing environmental flows after May. The choice of small reservoirs in series halves the impounded surface compared with an equivalent single dam, a strategy also recommended by [33] to reduce evaporative losses and sediment spread.

Adopting cascaded reservoirs, two structures up to 12 m high, linked in series, proved advantageous in terms of risk reduction, landscape integration, and proximity to agricultural blocks. This configuration is supported by regional analyses that demonstrate higher hydrological efficiency and lower evaporative losses per storage unit in networks of interconnected small reservoirs [34]. Only three sites (one with a downstream reservoir forming a cascade) met the hydraulic, geomorphological, and buffer-distance criteria in

São Brás. The selection applied all buffer zones simultaneously, considering distances from drainage networks, infrastructure, agricultural parcels, and protected areas. This approach ensured water availability and proximity to agricultural plots while minimising environmental impacts. These three sites collectively service 112 ha of agricultural plots by gravity and require embankments of $\leq$12 m. By contrast, the Dewana study identified 11 viable dams within the same watershed, allocating 5.55% of the basin to the "highly suitable" class and ranking alternatives with a weighted-product model (WPM), [35]. The larger portfolio in Dewana reflects the semi-arid topography (wider valleys, clayey lithology) and the inclusion of socio-economic layers such as distance to construction materials and archaeological sites, which our protocol purposefully excluded to retain hydrological parsimony.

In the study by Ullah et al. [36], site selection in Quetta combined a rule-based approach with a weighted multi-criteria evaluation, resulting in only 6.36 % of the area classified as "very high" and 25.35 % as "high." In São Brás de Alportel, where site selection was based exclusively on hydrological, geomorphological, and suitability criteria, only a small fraction of the territory was deemed suitable, further underscoring the scarcity of favourable locations.

In the present study, a monthly water balance was conducted to assess the water availability in the reservoirs of São Brás de Alportel. However, sedimentation was not considered, which will limit the reservoirs' efficiency over time. Studies, such as those by Bufalini et al. [37], indicate that some Italian reservoirs can lose more than 40% of their capacity within 50 years. This highlights the need to incorporate bathymetric monitoring and sediment management into future maintenance plans.

Drawing on the experience gained during this study, future work should (i) incorporate PlanetScope or drone imagery to refine intra-parcel mapping and calibrate crop coefficients; (ii) couple SWAT+ with hydrodynamic models that represent water-level variations in subbasins, exploiting synergies with radar-altimetry data; (iii) investigate floating covers or shading aerogenerators to reduce evaporation; and (iv) assess ecological-discharge regimes that minimise the loss of fine sediments. These actions could enhance water resilience in the face of the intensifying Mediterranean warming and rainfall variability scenario.

5. Conclusions

This study led to the following main findings:

Adequate water productivity: Catchment water productivity is sufficient to meet irrigation requirements in both average-rainfall year and dry year. Constructing small reservoirs, with a maximum water depth of 12 m behind simple embankments, secures supply during the summer months while enhancing the agricultural landscape.

Current extent of agricultural activity: The agricultural activity layer delineates 2854 ha (18.65% of the municipality), of which 112 ha (4%) are irrigated. The summer NDVI classification achieved a κ coefficient of 0.88, indicating an almost-excellent ability to identify irrigated parcels.

Hydrological baseline from the DEM: The DEM provided flow-direction and flow-accumulation models, from which a 758 km drainage network and 38 micro-catchments were delineated, forming the basis for site selection.

Reservoir location: Suitable dam points were identified on three streams that satisfied all technical criteria; for each, the contributing catchment area and the gravity-fed irrigated area (requiring no pumping) were calculated. It should be noted that site selection followed a rule-based approach, utilising exclusion buffers and suitability criteria, rather than a weighted multi-criteria evaluation, to ensure methodological simplicity and transparency.

Positive water balance in the average-rainfall year and in the dry year: The cumulative hydrologic balance is positive in an average year and in a dry year, assuming a maximum water depth of 12 m in the Mercês upstream reservoir, 10 m in the Alportel reservoir and 8 m in the Gaifona and Mercês downstream reservoir. The surplus justifies installing additional downstream reservoirs on the same watercourse, a viable option on the Ribeiras das Mercês.

Benefits of cascaded reservoirs: Cascades of small reservoirs, rather than a single large impoundment, minimise environmental and landscape impacts, distribute resources more evenly, and reduce hydrological risk.

Definition of the supply area: The supply area was limited to parcels intersecting the downstream watercourse, avoiding wastage. Introducing pumping could extend this area and diversify water use.

In summary, the GIS and remote sensing-based methodology proved effective for locating small-scale agricultural reservoirs, linking catchment areas, usable volumes, and irrigated areas. The approach is objective, replicable, and adaptable to other regions with comparable hydrological settings.

Author Contributions: Conceptualization, O.D. and C.C.; methodology, F.M.G.-M. and H.M.F.; software, O.D.; validation, C.O.S., R.L. and H.M.F.; formal analysis, R.L.; investigation, O.D.; resources, C.C.; data curation, O.D. and C.C.; writing—original draft preparation, O.D.; writing—review and editing, R.L. and H.M.F.; visualisation, F.M.G.-M.; supervision, R.L. and H.M.F. All authors have read and agreed to the published version of the manuscript.

Funding: This paper is financed by national funds provided by the FCT-Foundation for Science and Technology through project UIDB/04020/2020.

Institutional Review Board Statement: Not applicable.

Informed Consent Statement: Not applicable.

Data Availability Statement: Raw data is available upon request.

Conflicts of Interest: Author Olga Dziuba is employed by the company GeoPole. The remaining authors declare that the research was conducted in the absence of any commercial or financial relationships that could be construed as a potential conflict of interest.

References

1. Trnka, M.; Olesen, J.E.; Kersebaum, K.C.; Skjelvåg, A.O.; Eitzinger, J.; Seguin, B.; Peltonen-Sainio, P.; Rötter, R.; Iglesias, A.; Orlandini, S.; et al. Agroclimatic conditions in Europe under climate change. *Glob. Change Biol.* **2011**, *17*, 2298–2318. [CrossRef]
2. Rosa, A. *Rega das Culturas/Uso Eficiente da Água*; Direção Regional de Agricultura e Pescas do Algarve: Faro, Portugal, 2019.
3. Sutcliffe, J.V. *Hydrology: A Question of Balance*; International Association of Hydrological Sciences: Wallingford, UK, 2004, ISBN 978-1-901502-770.
4. Marengo, J.A. Água e mudanças climáticas. *Estud. Av.* **2008**, *22*, 83–96. [CrossRef]
5. Pedroso, A.V.A. Uso Eficiente da Água Num Edifício de Habitação. Master's Thesis, Instituto Superior de Engenharia de Lisboa, Lisboa, Portugal, 2014.
6. Rijo, M. A escassez da água e a sustentabilidade do regadio. In Proceedings of the 10º SILUSBA—Simpósio de Hidráulica e Recursos Hídricos dos Países de Língua Oficial Portuguesa, Porto de Galinhas, Brasil, 25–29 September 2011. Available online: http://hdl.handle.net/10174/3431 (accessed on 1 May 2025).
7. Gebeyehu, M.N. Remote sensing and GIS application in agriculture and natural resource management. *Int. J. Environ. Sci. Nat. Resour.* **2019**, *19*, 556009. [CrossRef]
8. Simón Sánchez, A.M.; González-Piqueras, J.; de la Ossa, L.; Calera, A. Convolutional neural networks for agricultural land use classification from Sentinel-2 image time series. *Remote Sens.* **2022**, *14*, 5373. [CrossRef]
9. Radulović, M.; Brdar, S.; Pejak, B.; Lugonja, P.; Athanasiadis, I.; Pajević, N.; Crnojević, V. Machine learning-based detection of irrigation in Vojvodina (Serbia) using Sentinel-2 data. *GISci. Remote Sens.* **2023**, *60*, 2262010. [CrossRef]
10. Yu, L.; Xie, H.; Xu, Y.; Li, Q.; Jiang, Y.; Tao, H.; Aihemaiti, M. Identification and monitoring of irrigated areas in arid areas based on Sentinel-2 time-series data and a machine learning algorithm. *Agriculture* **2024**, *14*, 1693. [CrossRef]

11. Melo e Silva, D. Integração de Ferramentas de SIG na Modelação Hidrológica de Pequenas Bacias Hidrográficas. Master's Thesis, Faculdade de Engenharia da Universidade do Porto, Porto, Portugal, 2008.
12. Machado, K.J.; Calijuri, M.L.; Ribeiro, C.A.A.S.; Santos, R.S.; Franco, G.B. Determinação automática da capacidade de armazenamento de um reservatório. *Rev. Bras. Cartogr.* **2010**, *62*, 43704. [CrossRef]
13. Lebon, N.; Dagès, C.; Burger-Leenhardt, D.; Molénat, J. A new agro-hydrological catchment model to assess the cumulative impact of small reservoirs. *Environ. Model. Softw.* **2022**, *153*, 105409. [CrossRef]
14. Aminzadeh, M.; Friedrich, N.; Narayanaswamy, S.; Madani, K.; Shokri, N. Evaporation loss from small agricultural reservoirs in a warming climate: An overlooked component of water accounting. *Earth's Future* **2024**, *12*, e2023EF004050. [CrossRef]
15. Villani, L. Participatory modeling of small reservoirs in the Orcia watershed, Italy. In Proceedings of the European Geosciences Union General Assembly 2024 (EGU24), Vienna, Austria, 14–19 April 2024; EGUsphere, EGU24-1011. [CrossRef]
16. Kottek, M.; Grieser, J.; Beck, C.; Rudolf, B.; Rubel, F. World map of the Köppen–Geiger climate classification updated. *Meteorol. Z.* **2006**, *15*, 259–263. [CrossRef] [PubMed]
17. Kopp, E.; Sobral, M.; Soares, T.; Woerner, M. *Os Solos do Algarve e as suas Características. Vista Geral*; DGEA-DRAA-GTZ: Faro, Portugal, 1989; 173p.
18. Rouse, J.W., Jr; Haas, R.H.; Schell, J.A.; Deering, D.W. *Monitoring the Vernal Advancement and Retrogradation (Green Wave Effect) of Natural Vegetation (No. NASA-CR-132982)*; NASA: Houston, TX, USA, 1973.
19. Portugal Diário do Governo. *Decreto-Lei N.º 44 647, de 26 de Outubro de 1962*; I Série Ed; Imprensa Nacional: Lisboa, Portugal, 1962.
20. Landis, J.R.; Koch, G.G. The measurement of observer agreement for categorical data. *Biometrics* **1977**, *33*, 159–174. [CrossRef] [PubMed]
21. Lencastre, A.C.; Franco, F.M. *Lições de Hidrologia*, 3rd ed.; Fundação da Faculdade de Ciências e Tecnologia da Universidade Nova de Lisboa: Caparica, Portugal, 2010; ISBN 9789728152590.
22. Agência Portuguesa do Ambiente (APA). *River Basin Management Plan for the Algarve Region (RH8)—3rd Planning Cycle 2022–2027*; Portuguese Environment Agency: Lisbon, Portugal, 2023. Available online: https://apambiente.pt/agua/3o-ciclo-de-planeamento-2022-2027 (accessed on 1 May 2025).
23. Agência Portuguesa do Ambiente (APA). Atlas do Ambiente. Available online: https://sniambgeoogc.apambiente.pt/getogc/rest/services/Atlas/Atlas_Ambiente/MapServer (accessed on 30 July 2025).
24. Sistema Nacional de Informação de Recursos Hídricos (SNIRH). Available online: https://snirh.apambiente.pt/index.php?idMain=2&idItem=1 (accessed on 30 July 2023).
25. Allen, R.G.; Perei7ra, L.S.; Raes, D.; Smith, M. *Crop Evapotranspiration—Guidelines for Computing Crop Water Requirements*; FAO Irrigation and Drainage Paper 56; Food and Agriculture Organization of the United Nations: Rome, Italy, 1998; pp. 63–74.
26. Município de São Brás de Alportel. Plano Diretor Municipal (PDM)—Áreas Urbanizáveis (Urbanizaveis_DGT_V2.jpg). Available online: https://cms.cm-sbras.pt//upload_files/client_id_1/website_id_1/servicos_mun/urbanismo/PDM/urbanizaveis_DGT_V2.jpg (accessed on 25 October 2025).
27. Instituto da Conservação da Natureza e das Florestas (ICNF). Zonas Especiais de Conservação (ZEC)—Serviço WFS. Available online: https://sig.icnf.pt/portal/home/item.html?id=a158877a57eb4f5fbad767d36e261fab (accessed on 25 October 2025).
28. Direção Regional de Agricultura e Pescas do Algarve (DRAPALG). Rede de Estações Meteorológicas Automáticas (EMA). Available online: https://www.drapalgarve.gov.pt/ema/ (accessed on 30 July 2023).
29. Hernández-López, D.; Aznar-Sánchez, J.A.; Gallego-Elvira, B.; Maroto-Morales, A. Mapping irrigated orchards in semi-arid Spain using multi-temporal Sentinel-1/2 imagery and random forests. *Remote Sens. Environ.* **2024**, *295*, 113592. [CrossRef]
30. Miranda Rodrigues, S.; Pereira, L.S.; Gonçalves, J.M. Evaporative losses from large reservoirs in Southern Europe: Current magnitude and future trends. *J. Hydrol.* **2020**, *588*, 125074. [CrossRef]
31. Rodrigues, L.; Miranda, R.I.; Pereira, S.L. Climate-change impact on evaporative losses from small Mediterranean reservoirs under CMIP6 scenarios. *J. Hydrol.* **2024**, *630*, 129024.
32. Montaldo, N.; Sarigu, A. Potential Links between the North Atlantic Oscillation and Decreasing Precipitation and Runoff on a Mediterranean Area. *J. Hydrol.* **2017**, *553*, 419–437. [CrossRef]
33. Alyami, S.H.; Jamil, R.; Ghanim, A.A. Feasibility Assessment and Environmental Benefits of Developing Rainwater Retention Ponds Across Najran Valley. *Arab. J. Sci. Eng.* **2024**, *49*, 14055–14069. [CrossRef]
34. Zhang, Y.; Gao, J.; Wang, X. Hydrological benefits of small-reservoir cascades in semi-arid regions. *Water Resour. Manag.* **2022**, *36*, 1321–1337.
35. Ahmad, B.A.; Salar, S.G.; Shareef, A.J. An Integrated New Approach for Optimizing Rainwater Harvesting System with Dams Site Selection in the Dewana Watershed, Kurdistan Region, Iraq. *Heliyon* **2024**, *10*, e27273. [CrossRef] [PubMed]

36. Ullah, S.; Iqbal, M.; Waseem, M.; Abbas, A.; Masood, M.; Nabi, G.; Tariq, M.A.U.R.; Sadam, M. Potential Sites for Rainwater Harvesting Focusing on the Sustainable Development Goals Using Remote Sensing and Geographical Information System. *Sustainability* **2024**, *16*, 9266. [CrossRef]
37. Bufalini, M.; Caruso, B.; Rinaldi, M. Bathymetric assessment of sedimentation rates in Italian small reservoirs. *Catena* **2022**, *213*, 106114. [CrossRef]